IOP Publishing Smart Materials and Structures
Smart Mater. Struct. **29** (2020) 073001 (25pp) https://doi.org/10.1088/1361-665X/ab8836

Topical Review

A review on shape memory alloy reinforced polymer composite materials and structures

Jitendra Bhaskar[1], **Arun Kumar Sharma**[1], **Bishakh Bhattacharya**[1] and **Sondipon Adhikari**[2]

[1] Department of Mechanical Engineering, Indian Institute of Technology Kanpur, Uttar Pradesh, India
[2] College of Engineering, Swansea University, Bay Campus, Fabian Way, Crymlyn Burrows, Swansea, SA1 8EN, United Kingdom

E-mail: bishakh@iitk.ac.in

Received 21 December 2019, revised 2 March 2020
Accepted for publication 9 April 2020
Published 2 June 2020

Abstract

Imparting controllable flexural rigidity into a material system is one of the key motivations for the design of intelligent materials for structural applications. In this direction, shape memory alloy (SMA) reinforced polymer composites have enormous potentials for active shape and vibration control of systems related to aerospace, automobile, and energy harvesting applications. The primary motivation of reinforcing SMA wires into a composite is to actively change the composite stiffness or elasticity through thermo-mechanical as well as electrical/magnetic stimulation. The SMA-reinforced hybrid composites are found to be able to adapt their shape, which may also improve the specific strength, vibration damping, and self-healing capability by utilizing shape memory effect and pseudoelastic behavior of the SMA. In this paper, we intend to provide a comprehensive review of all SMA-reinforced composites available today in the open literature and a critical assessment of the technology. Currently, shape memory alloys in the form of long fibers (wires), ribbons, short fibers, and particles are used for hybridizing the reinforcements in composites. Continuous SMA fiber embedded composites are generally used for shape control of structures. However, it has difficulty in obtaining suitable interfacial characteristics required for actuation. The discontinuous SMA embedded composites have scope for modifying such active properties. The work presented here gives an overview of the concepts of design, development, and modeling of continuous and discontinuous shape memory alloy embedded composites for advanced smart composites.

Keywords: smart composites, SMA hybrid composite (SMAHC), active fiber composite, ribbon-reinforced composite, active shape control, active vibration control.

(Some figures may appear in colour only in the online journal)

Nomenclature

α_f	Thermal expansion coefficient of the fiber	ν_m	Matrix volume fraction
α_m	Thermal expansion coefficient of the matrix	Ω	Phase transformation constant
ΔH	Enthalpy change	σ	Stress tensor
ν_A	Volume fraction of the austenite phase	σ_f^{cr}	Critical stress at the end of phase transformation
ν_f	Fiber volume fraction		

σ_s^{cr}	Critical stress at the start of phase transformation
σ_y	Yield stress of the matrix
$\square_\circ$	Subscript for initial state
$\square_{avg}$	Subscript for average
$\square_L$	Subscript for longitudinal direction
$\square_T$	Subscript for transverse direction
$\square_m$	Subscript for matrix
ε	Strain tensor
ε_L	Maximum recovery strain limit
ξ	Total volume fraction of martensite
ξ^s	Volume fraction of stress-induced detwinned martensite
ξ^T	Volume fraction of temperature-induced twinned martensite
ζ	Aspect ratio
A_f	Austenite finish temperature of SMA
A_s	Austenite start temperature of SMA
A_{surf}	Surface area
C_A	Stress rate for the austenite phase
C_M	Stress rate for the martensite phase
C_P	Specific heat
$d\sigma_{avg}^f$	Average incremental stress of SMA fiber
$d\sigma_{avg}^m$	Average incremental stress of the matrix
E_A	Modulus of elasticity of SMA in the austenite phase
E_f	Modulus of elasticity of fiber
E_M	Modulus of elasticity of SMA in the martensite phase
E_{avg}^m	Average modulus of elasticity of the matrix
h	Convection coefficient of ambient air
m	Mass of SMA wire
M_f	Martensite finish temperature of SMA
M_s	Martensite start temperature of SMA
$T(t)$	Instantaneous temperature at time t
T_a	Ambient temperature
V	Applied voltage to SMA wire

1. Introduction

Smart materials and structures have brought forth a paradigm shift in design mostly to the field of structural engineering, robotics, and aerospace due to which the demand for highly functional and lightweight, adaptive systems is continuously growing. Shape memory alloys (SMAs) belongs to the family of smart materials and have broad applications as components of adaptive structures [1] due to high specific actuation energy, immense actuation strain, and recovery stress. Shape memory effect (SME) and superelasticity are properties of SMAs that make them an ideal candidate for composite materials and smart composite structures. SME is realized as a shape deformation at low temperature (martensite phase) and shape recovery at high temperatures (austenite phase). Significant tensile stresses are induced in SMA if the recovery is constrained. Superelasticity can be described as a substantial recovery of strain upon deformation above the austenite finish temperature. SME can generate actuation stress in SMA in the range of 100–700 MPa, which is significantly higher as compared to low power hydraulic actuators (20–70 MPa) and piezoelectric actuators (1–9 MPa) [2]. There are about 20 varieties of SMA materials; however, NiTi-based, Cu-based (CuAlNi and CuZnAl), and Fe-based alloys are currently the most widely studied. In terms of commercial applications, NiTiNOL (a nickel-titanium alloy developed by Naval Ordnance Laboratory, White Oak, Maryland (USA), 1961) have gained wide popularity due to high performance, superior ductility, corrosion resistance, high tensile strength, large output force-to-weight ratio and bio-compatibility [3]. Ni-Ti-based SMAs can also be used as a sensor to measure the strain by utilizing the property of change of resistance during phase transformation [4]. There is another critical class of iron-based shape memory alloys that shows response under the magnetic field [5] known as ferromagnetic shape memory alloys (FSMAs) [6, 7]. FSMAs may be used as a magnetically sensitive device as well as a thermally sensitive one [8]. Shape memory alloys are widely employed in multiple domains of engineering to address an array of applications that are summarized in figure 1. These alloys can be used either as standalone or as a reinforcement in composites depending upon the application. The SMAs are commercially available in arrays of geometries such as wires, rods, ribbon, springs, foils, and even as foams [9]. The sintered NiTi alloy foam of high porosity (71–87%) are being investigated to match the actual performance of human bone [10].

Generally, pre-strained SMAs are employed such that upon heating above the austenite finish temperature, the material transforms back to its default dimensions as a consequence of recovery. With an increase in pre-strain, there occurs a parallel rise in stress associated with slip and dislocation movement [11]. As per ASTM E3098, the procedure followed for pre-straining the SMA has been outlined in figure 2.

In this paper, the attention is focused on the SMA-reinforced polymer composites. Polymer matrix-based composites materials with high-performance fibers such as carbon fiber, glass fiber, and Kevlar fiber have already been in use. The performance of these composites can be managed in various ways, such as the arrangement of reinforcing materials, curing, and by other external conditions (figure 3). The use of smart materials has created new ways to modify the mechanical properties of the composite. They can be reinforced with conventional advanced fibers for making hybrid composites. The concept of SMA-based hybrid composites (SMAHCs) was first proposed by Rogers *et al* [12]. Initially, SMAHCs were fabricated by reinforcing the SMA wires/strips in the epoxy matrix. SMAs were integrated with structure by bonding on the surfaces, either by directly embedding into the matrix [13] or reinforcing through the sleeves to govern the buckling of the host structure [14] (figure 4). Some of the parameters have been compared for sleeve-based and directly embedded SMA composites in table 1.

The actuation frequency from SMA can be achieved up to 100 Hz by increasing their surface area governing its bandwidth. With an increase in surface to volume ratio (SA/V ratio); the cooling performance (or response time) improves. With the same cross-sectional area, SA/V value concerning cylindrical configuration are 100%, 113%, and 132% for the cylinder, square prism, and rectangular prism, respectively.

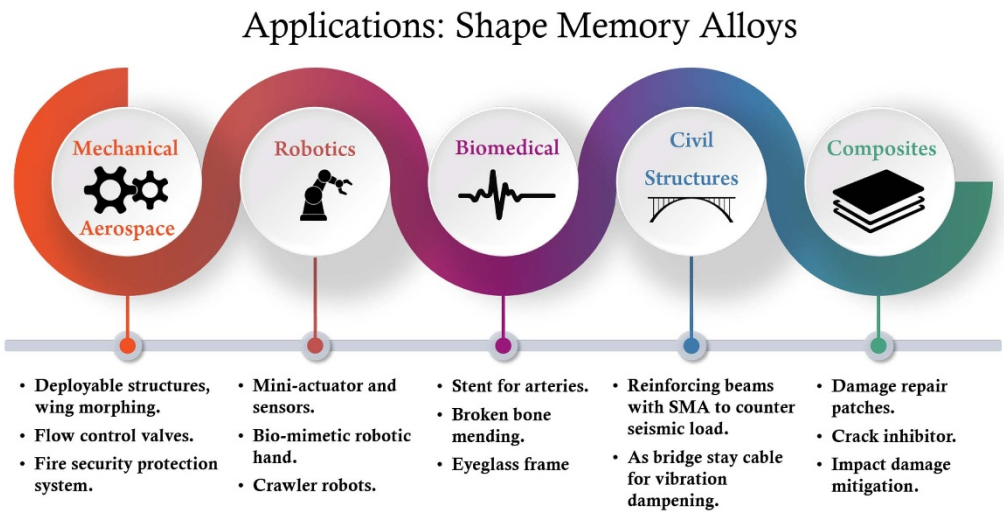

Figure 1. Application domain of shape memory alloys.

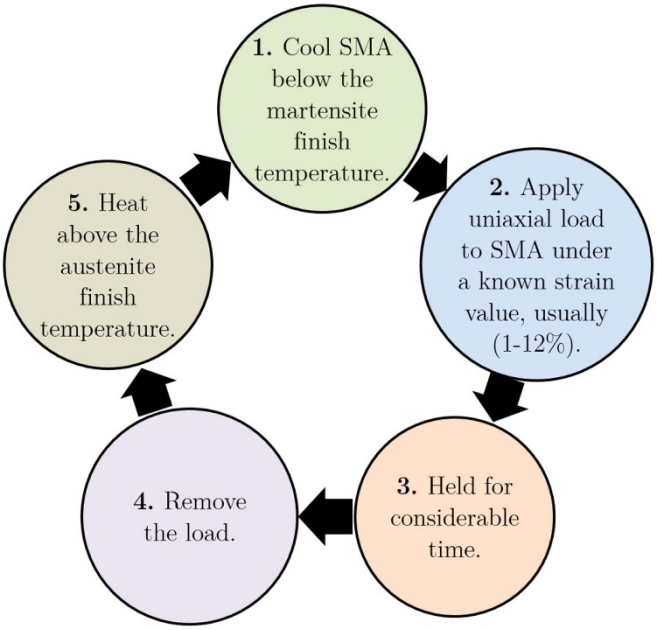

Figure 2. Procedure for pre-straining the shape memory alloys.

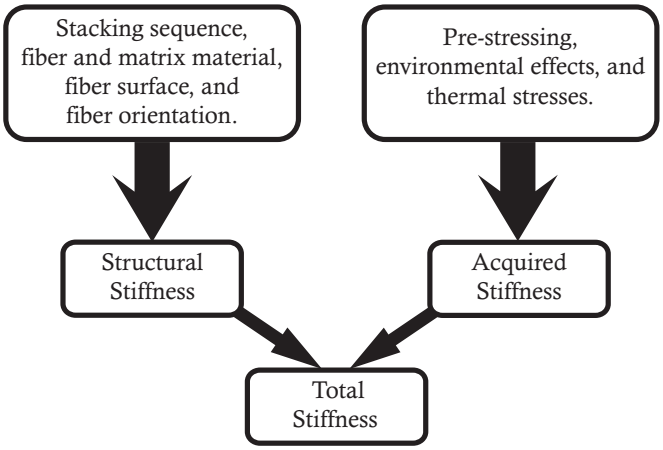

Figure 3. Key parameters controlling the structural and acquired stiffness of polymer matrix composite.

A significant rise in SA/V value can be attained from a thin material. However, there are manufacturing difficulties associated with the non-cylindrical form and may also reduce the fatigue life due to the sharp edges [16]. Thus, by linking of SA/V ratio to interfacial bonding, it is expected that more lateral surface area will provide better bonding with the matrix as well as heat transfer (cooling in case of resistive heating) from SMA to the matrix.

Thermoset-based polymer matrix composites are hybridized to improve the brittle nature of the matrix and low strain to failure characteristics. The hybridization with more robust fibers is also a design concept to design new hybrid composites to increase impact strength. The robust graphite fibers are utilized to augment the load-bearing capacity. The hybrid composite made of graphite/epoxy with Kevlar or S-glass fibers has shown moderate improvement in impact strength. However, the mechanical properties of graphite/epoxy composite may be improved significantly by hybridizing them with SMA fibers. Strain energies in common engineering materials such as Kevlar fiber, graphite, and glass fiber are in the range of 13 to 131 MJ/m^3, and metals such as aluminum and steel have strain energy at a yield in the range of 0.689 to 4.13 MJ/m^3. On the other hand, SMAs have the highest strain energy of about 127.5 MJ m^{-3}[17]. Polymer matrix-based advanced composites such as graphite/epoxy and glass/epoxy have enough potential to enhance the performance by integrating with SMA along with other fibers. SMA-reinforced polymer composite structures have been used for shape and position control, vibration control and acoustic properties, impact damage, and creep control in structures [18–20].

Mechanical properties of SMAHC and its structure depend upon the pre-strain of SMA, pre-treatment, the volume fraction of SMA, location of SMA with respect to the neutral plane, host matrix material, constraining condition of the matrix, as well as on the boundary conditions. A great variety

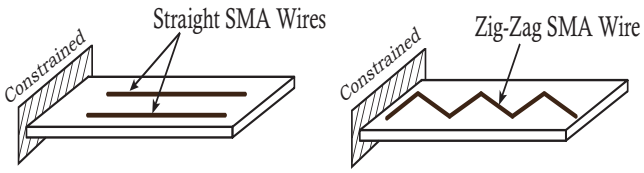

(a) SMA wires bonded on the composite plate in straight conguration and zig-zag arrangement [15].

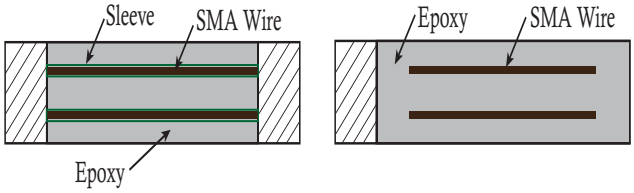

(b) SMA embedded into composite through sleeves and without sleeves.

Figure 4. Illustration of integration of shape memory alloy.

of SMA-based hybrid composites (SMAHC) is possible with the use of continuous SMA or discontinuous SMA. Continuous SMA fibers create higher strength and modulus in the fiber direction of composite and are generally weak in the transverse direction. Nevertheless, there are few drawbacks in embedding continuous SMA, such as interfacial failures on the actuation of SMA and high residual stress. The discontinuous SMAs are useful in dispersing the residual stresses in a composite. These can be economically fabricated using hand-layup techniques.

A vital aspect that limits the application SMA-based polymer composite is debonding at the SMA-matrix interface. The various methods [21] to enhance the bonding strength in such composites are summarized in table 2 along with relative capacities.

In this decade, many review papers have been published on application of shape memory alloy materials for shape morphing, applications, and opportunities [22–24]. The recent salient research areas concerning the SMA-embedded composite are summarized in table 3.

This review paper explores the design and fabrication of SMA embedded polymer composites related explicitly to continuous and discontinuous SMA-embedded polymer matrix composites and their characteristics. Section 2 discusses the shape memory effect and various prominent models governing the same. Section 3 presents various constitutive relations developed for SMA reinforced composites. Section 4 gives an overview of design parameters and issues associated with the fabrication of continuous SMA embedded polymer composites along with their applications. Section 5 discusses the fabrication techniques and engineering applications of discontinuous SMA-embedded composites. Section 6 explains the challenges associated with SMA-based polymer composites, and finally, the conclusions, along with certain directions for future work, are suggested in section 7.

2. Comprehensive review of shape memory alloy material

SMA displays properties of shape memory effect (SME) and superelasticity/pseudoelasticity. These properties are manifested by martensite (face-centered cubic (FCC) structure) and austenite phase (body-centered cubic (BCC) structure), which are interconvertible with each other under specific thermo-mechanical conditions. Shape memory effect, as shown in figure 5(a), is the ability of the material to recover the predefined shape without undergoing plastic deformation due to the change in a specific temperature range. SME is also known as an active mode of material since external energy is supplied to heat the material to reach austenite finish temperature and regain its parent configuration. SMA also have superelastic properties that are stress-dependent only. Here the material is in the austenite phase at room temperature, which upon loading transforms to stress-induced martensite and upon unloading transforms to austenite with strain recovery. SMA in the austenite phase, while undergoing cyclic stress, forms a hysteresis loop. Hysteresis can be regarded as an outcome of the movement of the twin boundaries. Phase transformations of SMA between austenite/martensite and between twinned /detwinned martensite are illustrated in figure 5(a) under various stress and temperature conditions. Internal friction is developed as a result of interface dislocation movements between the austenite and martensite phases. The co-existence of austenitic and martensitic phases are the source of damping in SMA.

The one-way SME is related to memorizing the shape at austenite phase (high temperature) only. Hence, the deformation imparted during the martensite phase is fully recovered upon heating, leaving no memory of the low-temperature phase, as evident from figure 5(b). Besides, the shape memory alloy also displays reversible or two-way SME by an

Table 1. Comparison between sleeve-based and directly embedded SMA composite.

Parameter	Sleeve-based	Directly embedded
Transfer of strain	No transfer of strain from SMA wire to matrix.	Transfer of strain from SMA wire to matrix.
	Strain in SMA is independent of the limitations of ply strain < 0.5%.	Due to the integrity of the host structure, ply strains of the composite are low with an elastic range of the SMA (0.5%).
	Modulus of composite is dependent upon temperature and strain.	Change in modulus from E_M to E_A is only dependent upon temperature.
Volume fraction and adhesion	Volume fraction is not limited as no dependency on adhesion.	Volume fraction is limited due to dependency on adhesion.
	No role of adhesion.	Maximum adhesion is needed.
Boundary conditions	Limited to fixed-fixed.	Not limited.
Mass Matrix	No contribution in mass matrix.	Contribution in mass matrix.
Natural frequency	Recovery force works against the constraint.	Recovery force against the matrix and natural frequency is affected significantly.
	Less recovery force is required for the same change in natural frequency.	More recovery force is required for the same change in natural frequency.
Suitability	Not feasible for rotating structures.	Feasible for rotating structures.

Table 2. Conventional surface treatment methods performed on SMAs to enhance bonding with a matrix in a composite.

Methods	Relative bonding enhancement
Torsion-induced roughness	+++++
Sandblasting	++++
Silane-based adhesives	+++
Electrochemical deposition	++
Hand sanding	++
Acid etching	+

appropriate combination of thermal and mechanical training. This enables the SMA to recall both high temperature (austenite phase) and low temperature (martensite phase) shapes. As a consequence, thus, just by varying the temperature, the material can achieve the trained shapes without the application of external load, as shown in figure 5(c). The various techniques to obtain two-way SME can be categorized as over-deformation, cool-deform-heat cycle, repeated pseudoelastic (PE) cycling, combined SME-PE cycling, constant strain-temperature cycling and are discussed in [35, 36].

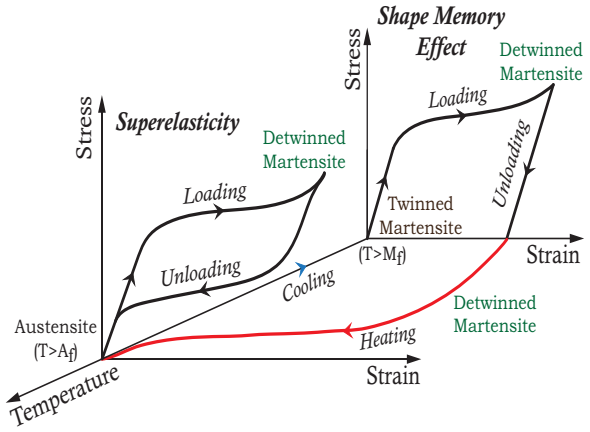

(a) Illustration of shape memory effect and superelastic behavior of SMA.

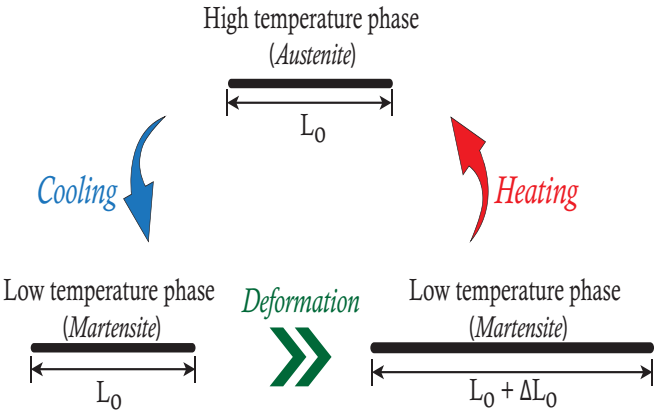

(b) One-way shape memory effect.

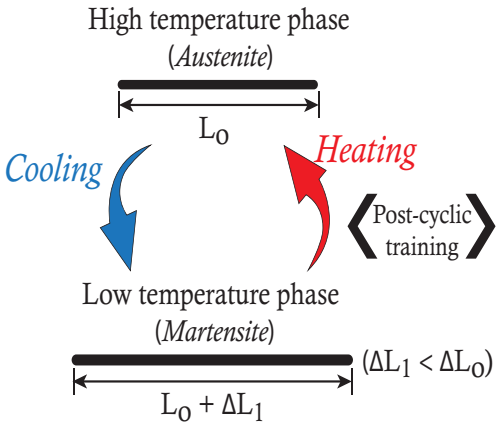

(c) Two-way shape memory effect.

Figure 5. Ilustration of behavior of the shape memory alloy.

Many phenomenological models developed for characterizing the thermomechanical behavior of SMA are summarized in table 4. Tanaka [37] (1986) proposed a 1-D model with martensite as a single internal variable and considered exponential function for variation of martensite fraction.

Table 3. Prominent research areas of SMA-embedded composites.

Research area	Utility
Bi-stable composite laminates	Shape morphing in aerospace structures, wind turbines, automobiles [25].
Electrochromism	Stretchable photonic crystal for dynamic camouflage such as anti-counterfeiting treatment, biomedicine [26].
SMA-bonding with composite matrix	Influence on deformation behavior of SMAs within the composite [27].
Marine Propellers	Improving the hydrodynamic efficiency using blade twist control [28].
Mechanical properties enhancement	Improving impact response, shape morphing and crack closure [29, 30].
Predicting actuation properties	Estimating actuation stroke and recovery of an SMA composite actuator [31].
Buckling response of composite shells	Predicting the amount of pre-strain and the number of embedded SMA wires to prevent buckling of thin walled shells [32].
Fatigue behavior	Fatigue failure mode and damage mechanisms [33].
Self-healing characteristics	Crack healing without the need of external force [34].

Material properties were assumed to be constant during the entire phase transformation. After a brief gap, Liang and Rogers [38] proposed cosine function, in place of an exponential function. Two internal variables, governed by cosine functions, were proposed by Brinson [39] for the transformation of twinned and detwinned martensite. Material properties were not constant during phase transformation. Boyd and Lagoudas [40] proposed a constitutive model based on free energy and heat dissipation ability. General plasticity was considered by Auricchio *et al* [41] for modeling pseudoelasticity and shape memory effect. Auricchio and Sacco [42] formulated the models for the internal variable concerning strain and temperature instead of stress and temperature, as proposed by previous scientists and engineers. Bekker and Brinson [43] formulated a model for possible paths with cosine functions for phase transformation in stress-temperature space.

2.1. Modelling with multiple martensites

Figure 6 illustrates the stress-temperature phase diagram concerning the Brinson model [39]. At the temperature-axis, the intercept of lines represents the transformation temperature at zero stress condition. There are regions on the graph that represent the pure phase and co-existence of multiple phases. It is assumed that transformation temperature varies linearly with stress. The stress influence coefficients (C_M and C_A) symbolizes the slopes of martensite and austenite phase lines, respectively, and the influence of stress on the shifting of transformation temperatures. The critical stress corresponding to the start of transformation (from 100% twinned martensite) to the finish are represented by σ_s^{cr} and σ_f^{cr}, respectively. The behavior of SMA is dependent upon the multiple martensite volume fractions. There are two types of martensite, one is stress-induced de-twinned martensite (ξ^s), and the other temperature-induced twinned martensite (ξ^T). So, the total martensite volume fraction can be expressed as follows.

$$\xi = \xi^s + \xi^T. \tag{1}$$

Stress-induced de-twinned martensite (ξ^s) is a function of stress and temperature.

Brinson proposed the stress in terms of stress-induced martensitic volume fraction following the below equations.

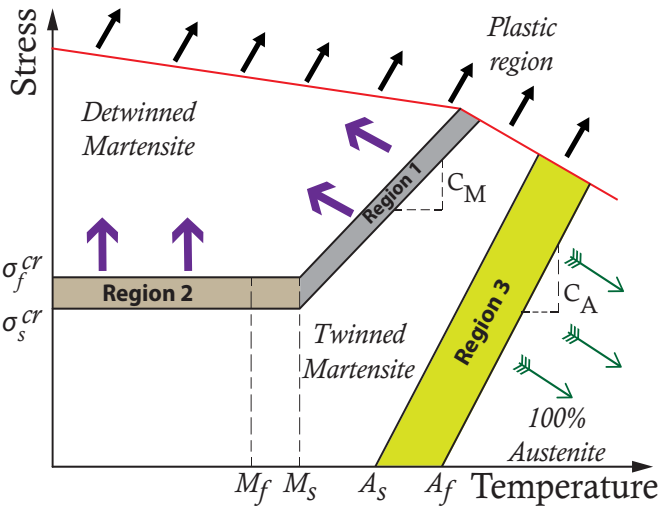

Figure 6. Illustration of transformation behavior of SMA with stress and temperature in accordance with the Brinson model.

$$\sigma - \sigma_\circ = E(\varepsilon - \varepsilon_\circ) + \Omega\left(\xi^s - \xi_\circ^S\right) + \theta(T - T_\circ) \tag{2}$$

where $(\sigma_\circ, \varepsilon_\circ, T_\circ, \xi_\circ)$ represent the initial state and Ω is the transformation coefficient, θ is thermal expansion coefficient and E is the modulus of elasticity calculated using the rule of mixture as

$$E\{\xi\} = E_A + \xi(E_M - E_A)\,. \tag{3}$$

Transformation coefficient can be defined as

$$\Omega = -\varepsilon_L E \tag{4}$$

where, ε_L is the maximum residual strain.

Conversion to detwinned martensite

For T > M_s (region 1 in figure 6),

$$\sigma_s^{cr} + C_M(T - M_s) < \sigma < \sigma_f^{cr} + C_M(T - M_s)$$

$$\xi^S = \frac{1 - \xi_\circ^s}{2} \times \cos\left[\frac{\pi}{\sigma_s^{cr} - \sigma_f^{cr}}\left\{\sigma - \sigma_f^{cr} - C_M(T - M_s)\right\}\right] + \frac{1 + \xi_\circ^s}{2}$$

Table 4. Features of prominent SMA models.

Authors	Features
Tanaka [44]	Young's modulus, $E = E_A = E_M$
Sato and Tanaka [45], Liang and Rogers [38]	Martensite and austenite phases are operating in parallel along the wire. Elastic modulus, $E(\xi) = \xi E_M + (1-\xi)E_A$
Ivshin and Pence [46] Auricchio *et al* [47]	Martensite and Austenite phase are operating in series. Elastic Modulus, $E(\xi) = \frac{E_A E_M}{\xi(E_A - E_M)+E_M}$
Brinson [39]	Martensite fraction is divided into temperature-induced and stress- induced parts.
Bekker and Brinson [43]	Described martensite fraction transformation due to thermomechanical loading.
Aurricchio *et al* [48]	For temperature higher than M_s, only austenite and single variant martensite is considered. This single variant martensite was taken as a single independent variable.
Nallathambi *et al* [49]	Proposed thermodynamically dependent three-phase model: austenite, plus-martensite and, minus-martensite.
Marfia and Rizzoni [50]	Studied the axial and bending behavior considering different behavior in tension and compression.

E_A - Modulus of austenite
E_M - Modulus of martensite
ξ- Martensite volume fraction.

$$\xi^T = \xi_\circ^T - \frac{\xi_\circ^T}{1-\xi_\circ^S}(\xi^s - \xi_\circ^S). \tag{5}$$

For T < M$_s$, $\sigma_s^{cr} < \sigma < \sigma_f^{cr}$ (region 2 in figure 6)

$$\xi^s = \frac{1-\xi_\circ^s}{2} \times \cos\left[\frac{\pi}{\sigma_s^{cr} - \sigma_f^{cr}}(\sigma - \sigma_f^{cr})\right] + \frac{1+\xi_\circ^S}{2}. \tag{6}$$

Expression for calculating ξ^T as in the Brinson model was modified by Sayyaadi *et al* [51]

$$\xi^T = \Delta_{T_\varepsilon} - \frac{\Delta_{T_\varepsilon}}{1-\xi_\circ^s}(\xi^s - \xi_\circ^S). \tag{7}$$

Here, if $M_f < T < M_s$ and $T < T_\circ$

$$\Delta_{T_\varepsilon} = \frac{1-\xi_\circ^S - \xi_\circ^T}{2}\cos\left[a_M(T - M_f)\right] + \frac{1-\xi_\circ^S + \xi_\circ^T}{2}$$

where, $a_M = \left(\frac{\pi}{M_s - M_f}\right)$
else, $\Delta_{T_\varepsilon} = \xi_\circ^T$.

Conversion to austenite

For T > A$_s$,

$C_A(T - A_f) < \sigma < C_A(T - A_s)$ (region 3 in figure 6)

$$\xi = \frac{\xi_\circ}{2}\left\{\cos\left[a_A\left(T - A_s - \frac{\sigma}{C_A}\right)\right] + 1\right\} \tag{8}$$

where $a_A = \left(\frac{\pi}{A_f - A_s}\right)$

$$\xi^s = \xi_\circ^s - \frac{\xi_\circ^s}{\xi_\circ}(\xi_\circ - \xi) \tag{9}$$

$$\xi^T = \xi_\circ^T - \frac{\xi_\circ^T}{\xi_\circ}(\xi_\circ - \xi) \tag{10}$$

where $\xi_\circ^s$ and $\xi_\circ^T$ are the initial stress-induced and temperature-induced martensite volume fractions.

2.2. Constitutive relations in differential form

Stress increment in SMA fiber is expressed in terms of deformation under the elastic limit, change in stress-induced martensitic ($d\varepsilon^s$) and thermal expansion (α_f) as below [52].

$$d\sigma_f = E_f d\varepsilon_f - \varepsilon_L E_f d\xi^s - E_f \alpha_f dT \tag{11}$$

where E_f and α_f are non-constant material functions depending upon martensite volume fractions.

$$E_f(\xi) = (1-\xi)E_A + \xi E_M \tag{12}$$

$$\alpha_f(\xi) = (1-\xi)\alpha_A + \xi\alpha_M. \tag{13}$$

For shape control, strain is made as an independent variable as given below:

$$d\varepsilon_f = \frac{1}{E_f}d\sigma_f + \varepsilon_L d\xi^s + \alpha_f dT. \tag{14}$$

Stress-induced martensite depends on stress and temperature, and volume fraction (ξ^s) can be expressed as;

$$d\xi^s = \frac{\partial \xi^s}{\partial \sigma_f}d\sigma_f + \frac{\partial \xi^s}{\partial T}dT. \tag{15}$$

Replacing ($d\xi^s$) into equation (11)

$$d\sigma_f = \frac{E_f}{1 + \varepsilon_L E_f \frac{\partial \xi^s}{d\sigma_f}}\left[d\varepsilon_f - \left(\varepsilon_L \frac{\partial \xi^s}{\partial T} + \alpha_f\right)dT\right]. \tag{16}$$

Strain in SMA by replacing ($d\xi^s$) into equation (14)

$$d\varepsilon_f = \left(\frac{1}{E_f} + \varepsilon_L \frac{\partial \xi^s}{\partial \sigma_f}\right)d\sigma_f + \left(\varepsilon_L \frac{\partial \xi^s}{\partial T} + \alpha_f\right)dT. \tag{17}$$

Heat transfer formulation:

SMAs can be activated through Joule heating by applying voltage (V) for actuator applications. For mathematical formulations, only heat dissipation by convective heat transfer (h),

heat capacity (C_p) and heat correlated to enthalpy (ΔH) for the phase transformation (martensite to austenite) have been considered for simulating the temperature of the SMA as below [53, 54]:

$$\frac{V^2(t)}{R_w} = hA_{sur}\{T(t) - T_a\} + mC_p\frac{dT}{dt} + m\Delta H \tag{18}$$

where R_w, T_a and m are electrical resistance, ambient temperature and mass of the wire, respectively. The resistance of SMA wire is dependent upon volume fractions of martensite and austenite.

The cooling of SMA after Joule heating can be expressed as

$$hA_{sur}\{T(t) - T_a\} + mC_p\frac{dT}{dt} + m\Delta H = 0. \tag{19}$$

3. Constitutive relations for SMA reinforced composite

Rogers and Robertshaw [55] proposed the concept of embedding the SMA in composites. The behavior of SMA-reinforced composites depends upon the interaction of SMA with matrix in the following situations:

1. Without the recovery of SMA: only active modulus
2. With constrained/restrained recovery of SMA with temperature: SME effect
3. With constrained/restrained recovery of SMA at constant (higher) temperature: pseudoelasticity effect

Analysis of SMA-embedded composites is quite complex due to the involvement of micromechanics and nonlinearity. The behavior of the SMA composite may be simulated by using composite constitutive relations based on the volume fraction of SMA and matrix. Properties of SMA are obtained for the volume fraction of martensite in SMA by the rule of mixture. Numerous micromechanical methods are available to predict the behavior of SMA or SMA-embedded composites [56]. Sullivan [57] proposed the model for unidirectional SMA composites, and Birman *et al* [58] proposed a model using a micromechanical approach. However, these micromechanical approach-based models are difficult to implement. A simplified model following the macromechanics approach was developed by Turner [59], based upon experimental measurements of basic engineering properties. Various models governing the response of continuous SMA-reinforced composites are tabulated in table 5.

3.1. Constitutive relation for continuous SMA fiber-reinforced composite

The increment in stress for a long fiber SMA composite can be manifested by the rule of mixture [52] as

$$d\sigma = \nu_f d\sigma_f + (1 - \nu_f)d\sigma_m. \tag{20}$$

The subscript *'f'* denotes SMA fiber.

Constitutive relation for elastic matrix,

$$d\sigma_m = E_m d\varepsilon_m - E_m\alpha_m dT. \tag{21}$$

By substituting equation (16) and equation (21) into equation (20), the incremental constitutive relation for the long SMA fiber inelastic matrix composite can be obtained as follows:

$$d\sigma = \left\{(1-\nu_f)E_m + \frac{\nu_f E_f}{\left(1+\varepsilon_L E_f\frac{\partial\varepsilon^s}{\partial\sigma_f}\right)}\right\}d\varepsilon - \left\{(1-\nu_f)E_m\alpha_m + \frac{\nu_f E_f\left(\varepsilon_L\frac{\partial\varepsilon^s}{\partial T} + \alpha_f\right)}{\left(1+\varepsilon_L E_f\frac{\partial\varepsilon^s}{\partial\sigma_f}\right)}\right\}dT \tag{22}$$

where the incremental strains of the composite, fiber and matrix have the following relationship:

$$d\varepsilon = d\varepsilon_f = d\varepsilon_m. \tag{23}$$

3.2. Constitutive relation for short-fiber reinforced composite

Mathematical models based on a micromechanical approach known as the inclusion method of Eshelby [67] are developed for SMA-embedded composites with an inelastic or plastic polymer matrix. Wang *et al* [68] proposed a micromechanics-based model for short SMA composites with an elastic epoxy polymer matrix (table 6). The authors developed an equivalent inclusion model for composites reinforced with SMA short fibers of the same size aligned along the axis. The model was used to predict the transformation strain coefficient and the thermal expansion coefficient. All the previous works for short SMA composites indicate that Eshelby's inclusion model with models of SMA constitutive relations is a powerful method for investigating short fiber composites. Wang *et al* [68] also emphasized the role of aspect ratio and fiber volume fraction of short fibers on the mechanical response. For $M_s < T < A_s$ and $T > A_f$, the stress-strain curves of the SMA composites were similar to SMA fiber. There was a difference in the behavior of SMA fiber and SMA composites during unloading in temperature range $A_s < T < A_f$. At high aspect ratio, the performance of short SMA-based composites was very similar to SMA when the volume fraction of SMA escalated. Critical stresses were enhanced with an increase in SMA volume fraction, except austenite start stress. Phase transformation zones were also squeezed as the fiber volume fraction increased. The equivalent properties of the composites were dominated by fiber volume fraction than the fiber aspect ratio. Overall mechanical response of the composite was appreciable at aspect ratio above ten. Lei *et al* [69] investigated the effect of the unidirectional random distribution of SMA short fibers based on Eshelby's equivalent inclusion and the Mori-Tanaka scheme. Three-phase equivalent system and two-step equivalent process were considered for evaluating the elastic

Table 5. Comparison of proposed models for continuous SMA-reinforced composites.

Authors / year	Modelling Approach	Material	Details
Boyd and Lagoudas [56]	Mori-Tanaka	Elastomer matrix composites	For unidirectional fiber. Considered for transformation temperatures, thermal expansion coefficient and transformation strain coefficient.
Ostachowicz *et al* [60]	FEM	8-layered carbon-epoxy plate	Numerical simulations for evaluating the effect of SMA fibers on natural frequency of SMA embedded composite.
Turner [59]	Equivalent thermal expansion coefficient	Graphite epoxy	Recovery stress was calculated using this CTE over a temperature range. Buckling analysis and dynamic analysis was performed.
Balapgol *et al* [61]	No variants of martensite	GFRP, elastomers	A non-linear FEM for free vibration analysis of laminated composites thermally actuated. Vibration is more affected by the position of SMA from neutral axis.
Sharma *et al* [62]	Variational asymptotic analysis for self-healing	CFP and SMA	Four layered composite lamina was analyzed using variational asymptotic analysis for self-healing of the composite. Wire size was optimized without compromising the crack closure force for healing.
Ryu *et al* [63]	Elastic prediction transformation correction method was used for martensite volume fraction.	GFRP with SMA and silicon rubber	Numerical simulation and experimental study for compliant material such as silicon rubber for improving more achievable deformation.
Cho and Rhee [64]	Nonlinear FEM	SMA epoxy	Simulation of SMA-reinforced graphite composites.
Khalili *et al* [65]	Concepts of 2D spring-mass system and linearized contact law	CFRP and GFRP	The effect of embedding SMA wires into laminated CFRP and GFRP beams on the impact behavior was studied.
M. Chang *et al* [66]	Modified Hashin failure criterion, Brinson model, and a visco-hyperelastic model.	SMA-reinforced glass fiber/epoxy composites	Numerically studied the impact resistance at varying frequencies and amplitudes.

modulus and thermal expansion coefficient. The high aspect ratio was dominant for elastic modulus.

Based on the incremental approach to stress and temperature, Murasawa *et al* [52] proposed a model for short SMA composite based on a shear lag model considering the interaction between the fibers and matrix. In this model, short SMA fibers were aligned along the direction of load application, as shown in figure 7. This can be visualized as two-cylinder configuration in which the homogenized matrix (length L, diameter D) encloses a short SMA fiber (length l, diameter d). It was assumed that the incremental deformation in both matrix and fiber is linear, and the material properties are a function of average stress. Upon application of load, the tensile and shear stresses are induced in fiber and at the fiber-matrix interface, respectively.

The distribution of the incremental stress along the fiber in terms of average stress in the short fiber can be expressed as

$$d\sigma_f = \frac{E_f}{1+\varepsilon_L E_f \frac{\partial \xi^S_{avg}}{d\sigma^f_{avg}}} \left\{ d\varepsilon - \left(\varepsilon_L \frac{\partial \xi^S_{avg}}{\partial T} + \alpha_f \right) dT \right\} C \quad (24)$$

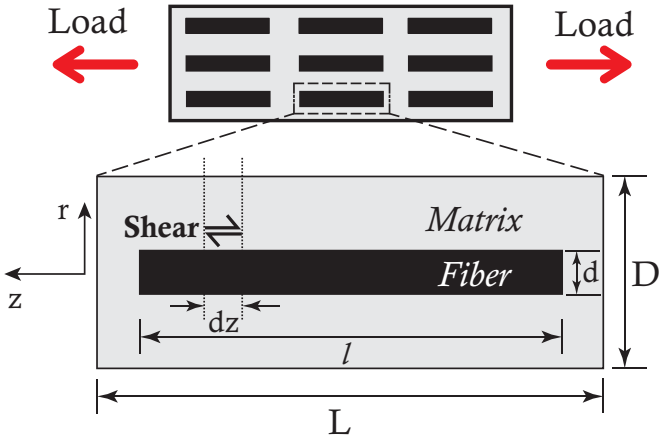

Figure 7. Configuration of the shear-lag model for aligned short fiber-reinforced composites [52].

where 'C' is a function of average stress in SMA, the geometry of SMA fiber, recovery strain limit and modulus of SMA.

The incremental stress of the short fiber SMA composite is expressed by the rule of mixture

Table 6. Comparison of proposed models for short SMA fiber-reinforced composites.

Authors	Modelling approach	Material	Details
Wang *et al* [68]	Eshelby's model and Mori-Tanaka	Epoxy matrix with aligned short SMA	Predicted the effect of SMA volume fraction and aspect ratio on transformation critical stress of composites.
Murasawa *et al* [52]	Elasto-plasticity and Shear-lag model	Polycarbonate	Simulated the behavior of short SMA fiber embedded polycarbonate composites.
Zhang *et al* [70]	Halpin-Tsai model	Epoxy resin with Short SMA fiber or SMA particles.	Flexural properties and dynamic mechanical properties were simulated and experimentally investigated.
Lei *et al* [69]	Eshelby model and Mori-Tanaka approach	Unidirectional random distribution of SMA in epoxy	Calculated elastic modulus and thermal expansion coefficient. The failure occurs due to debonding of interface and SMA in short fiber reinforced composites.
Lei *et al* [71]	Cohesive zone model	Superelastic NiTi alloy in epoxy resin.	Investigated the shear and ultimate strength at the fiber-matrix interface on the basis of tensile tests aided by the Monte-Carlo method.
Khalili *et al* [72]	Representative volume element method (RVE) with modelling of interface region using Cohesive zone model.	Epoxy matrix with straight and oblique short SMA.	Mechanical properties was reduced for low aspect ratio. Reduction of 9% in the axial modulus and enhancement of 10% in transverse was found for 15° oblique wires.
Khalili and Saeedi [73]	RVE with the Eshelby model and Mori Tanka approach.	Epoxy matrix with randomly oriented pre-strained short SMA fiber with aspect ratio upto 35.	Predicted elastic properties of composite. Elastic modulus was improvedby 20% and 12% due to aspect ratio and pre-strain, respectively.

$$d\sigma = \nu_f d\sigma^f_{avg} + (1-\nu_f) d\sigma^m_{avg} \tag{25}$$

where $d\sigma^f_{avg}$ and $d\sigma^m_{avg}$ are the average incremental stress of the SMA fibers and matrix, respectively. ν_f is the volume fraction of SMA fibers of length 'l' in the composite.

$$d\sigma^f_{avg} = \frac{2}{l}\int_0^{l/2} (d\sigma_f) dz$$

$$d\sigma^f_{avg} = \frac{E_f^{'}}{1+\varepsilon_L E_f \frac{\partial \xi^S_{avg}}{d\sigma^f_{avg}}} \left\{ d\varepsilon - \left(\varepsilon_L \frac{\partial \xi^S_{avg}}{\partial T} + \alpha_f \right) dT \right\} \tag{26}$$

where $E_f^{'}$ is a function of average SMA modulus and constant 'C' as in equation (24).

Substituting the incremental strain in the composite into the constitutive equation of matrix equations, the average incremental equation of the matrix can be written as:

$$d\sigma^m_{avg} = E^m_{avg} d\varepsilon - E^m_{avg} \alpha_m \, dT. \tag{27}$$

Hence, the incremental constitutive equation for short fiber SMA elastic matrix composite can be drafted by substituting equation (26) and equation (27) into equation equation (25) as follows.

$$d\sigma = \left\{ (1-\nu_f) E^m_{avg} + \frac{\nu_f E_f^{'}}{\left(1+\varepsilon_L E^f_{avg} \frac{\partial \xi^S_{avg}}{d\sigma^f_{avg}}\right)} \right\} d\varepsilon$$

$$- \left\{ \left\{ (1-\nu_f) E^m_{avg} \alpha_m + \frac{\nu_f E_f^{'} \left(\varepsilon_L \frac{\partial \varepsilon^s}{\partial T} + \alpha_f \right)}{1+\varepsilon_L E^p_{avg} \frac{\partial \xi^S_{avg}}{\partial \sigma^f_{avg}}} \right\} dT. \right. \tag{28}$$

Numerical analysis was performed for several volume fractions in the range of 5% to 30% for the aspect ratio of 10. In another case, the aspect ratio was varied from 5 to 25 for the volume fraction of 4%. Initially, there were residual stresses in the composite due to loading and unloading. In the absence of residual stress, internal stress and deformation of the composite were intensified in the composite before heating. The aspect ratio has a very small effect on both of these. However, the transformation temperature of short SMA fiber was found to be changing with aspect ratio.

3.3. Storage modulus and loss factor of short SMA circular fiber embedded layer

The elastic modulus for discontinuous unidirectional fiber-reinforced composites can be obtained using the Halpin-Tsai

equation [74, 75]. The modulus of fiber-reinforced polymer matrix composites in the longitudinal (E_L) and transverse direction (E_T) can be expressed as

$$E_L = \frac{E_m(1+2\zeta\eta_L\nu_{SMA})}{1-\eta_L\nu_{SMA}}, \tag{29}$$

$$E_T = \frac{E_m(1+2\zeta\eta_T\nu_{SMA})}{1-\eta_T\nu_{SMA}}, \tag{30}$$

where ν_{SMA} is a volume fraction of SMA wire, L and D are the lengths of SMA short fiber and diameter of SMA wire, aspect ratio, $\zeta = \frac{L}{D} = 2$ for the circular cross-section and E_m is the polymer matrix modulus.

The parameters η_L and η_T in the above equations represents

$$\eta_L = \frac{\left(\frac{E_{SMA}}{E_m}\right)-1}{\left(\frac{E_{SMA}}{E_m}\right)+2\zeta}; \eta_T = \frac{\left(\frac{E_{SMA}}{E_m}\right)-1}{\left(\frac{E_{SMA}}{E_m}\right)+2}. \tag{31}$$

Modulus of SMA composite with randomly oriented discontinuous fibers in two dimensions can be expressed as:

$$E_C = \frac{3}{8}E_L + \frac{5}{8}E_T. \tag{32}$$

4. Continuous SMA embedded polymer composites

Continuous SMAs are readily available commercially in distinct configurations, such as wires, ribbons, and even thin films. Using these forms of SMA, a great diversity of SMA hybrid composites can be designed and fabricated using conventional composite fabrication procedures along with additional fixtures for embedding the SMA fiber. Continuous SMA wires were embedded in the polymer matrix [76] composites with carbon fiber [77, 78], glass fiber [77, 79, 80], Kevlar fiber composites [81–84]. The SMA ribbon was embedded with glass fibers [85]. Detailed features of continuous SMAHC are discussed in the following sections.

4.1. Design parameters

SMA-based composite design is primarily dependent upon the properties of the matrix and SMA fiber and the corresponding volume fractions, as shown in figure 8. SMAs have both active and passive properties. Active and passive SMA composites are designed with SMAs based on shape memory effect and pseudoelastic properties, respectively. In the passive mode, the SMA fibers are inserted to strengthen the PMC, store strain energy, and increase the residual stress by inhibiting the crack propagation. In an active mode, the SMAs in composites are actuated either by heating the SMA in a high-temperature environment or by resistive heating of SMA. The phase transformation begins above the austenite start temperature, which increases the stiffness. The recovery stresses generated by the SMA wires depend upon the compliance of the surrounding matrix in a direct embedding situation. The low compliance of matrix permits us to induce a high level of shear force. Due to resistive heating, SMA shrinks and therefore generates a large shear force (tension/compression) along the longitudinal dimension. These shear loads affect the stiffness, vibrational behavior, and shape of the composite.

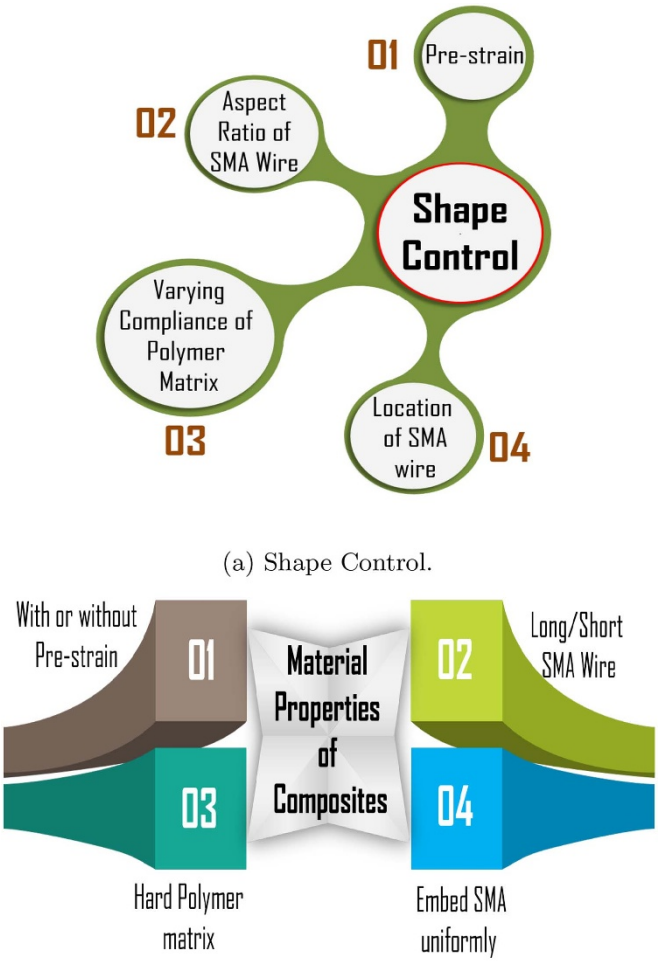

Figure 8. Schematic representation of important parameters in SMA-embedded polymer composite for achieving shape control and desired material properties.

Directly embedding the SMA within the polymer matrix leads to the situation of overheating and damage to the matrix. Hence, it is preferred to embed SMA through sleeves allows creating insulation with the surrounding matrix. There are various factors such as constraining matrix, level of pre-strain, interfacial bonding, the arrangement of SMA, and size of SMA, which affects the levels of compressive stresses SMAHC during heating. However, by directly embedding SMA into composites, various actuation and sensing functionality can be imparted to the polymer composites. There are two techniques to modify properties of SMA-based hybrid composites while using shape memory effect of SMA in active mode as given below [12]:

1. **Active Property Tuning (APT)**: In this technique, the SMA without plastic deformation is incorporated to raise the stiffness of the hybrid composite. The change in stiffness is due to change in modulus of SMA with the transformation of martensite into austenite directly, without transforming into detwinned martensite.
2. **Active Strain Energy Tuning (ASET)**: In this technique, the SMA with plastic deformation is used for embedding into polymer composites. Detwinned martensite phase is available in plastically deformed SMA. Pre-strained SMA tries to recover its shape that produces the internal forces.

Active property tuning (APT) increases the modulus of elasticity and tensile strength. There is an appreciable requirement of volume fraction of unstrained SMA. Internal forces are not produced with the unstrained. However, Active strain energy tuning (ASET) is beneficial due to the use of pre-strained SMA. A smaller volume fraction of SMA fiber is desired in ASET. Significant internal compressive stresses are generated throughout the structure. In passive application, there is no need for external energy/stimulation required for the actuation of superelastic SMA wire in which austenite finish temperature is close to ambient temperature. Stress-induced transformation occurs in SMA, and polymer composite deforms under stress and tries to return to the original shape when the load is released partially. The damping effect in polymer composites is enhanced due to superelasticity. In the early phase of SMA-based smart composites, weaving SMA wires have been reported by using the woven SMA fabric of SMA wires of 150 μm in diameter [86]. For instance, by assimilating SMAs into conventional glass/carbon fibers, various multifunctional properties can be imparted to a section of textile fabric.

4.1.1. Effects of the constraining matrix. The constraining matrix plays a crucial role in improving the functional properties of the SMAHC. The polymer matrix constrains long SMA fibers. Constrained SMA in continuous configuration works against the stiffness of the matrix. Psarras *et al* [87] described the importance of the secure interface between the SMA wire and matrix. Interfacial bonds should be strong enough so that stresses could be transmitted to the matrix material. Jonnalagadda *et al* [88] observed that SMA-polymer adhesion was a good source of increasing the bond strength, enhancing the interfacial shear stress induced in the matrix.

4.1.2. Effects of pre-strain and volume fraction on the recovery force. The recovery forces are generated by the SMA while regaining its pre-strained elongation under temperature higher than austenite start temperature [89]. These forces are proportional to the pre-strain of the single element of SMA. The total recovery force corresponds to the volume fraction of SMA within the composite. The recovery of stress was slower at high pre-strained value. An appreciable amount of SMA volume fraction is essential for an observable recovery force. Residual stresses in the composite are generated due to the curing of the thermoset polymer. Psarras *et al* [87] observed that with the rise in SMA volume fraction, the residual compressive stress diminishes. Generally, SMAs are fixed in a frame to stop contraction of the wire during curing of the thermoset polymer matrix of the composite. In this situation, the tensile stresses are developed and transmitted to the neighboring fibers. Aoki *et al* [90] experimented with epoxy resin matrix beams with embedded reinforced Ti-Ni SMA fibers. The high volume fraction of SMA into composite results in the weakening of interfacial bonding and also induces matrix cracking, delamination, and de-bonding between the SMA and matrix under bending test [91].

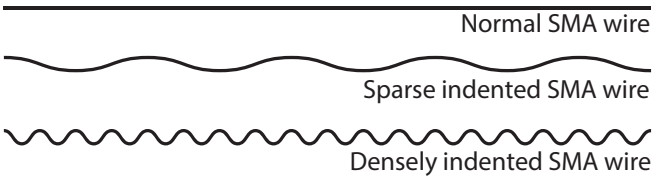

Figure 9. Configuration of indented SMA wires.

4.1.3. Interfacial bonding. Interfacial bonding in SMA embedded composite is responsible for effective load transfer through SMAHC. Generally, such composites have the limitation of the weak interface between the SMA fiber and matrix [91]. Jonnalagadda *et al* [92] applied surface treatments such as acid etching, hand sanding, sandblasting, plasma treating, and silane coating on the NiTiNOL wires to investigate the load transfer from SMA to the polymer matrix. It has been observed that bond strength enhanced by 189% due to sandblasting over the untreated wire. Ogisu *et al* [93] used 10% NaOH to treat the carbon fibers for CFRP. Epoxy adhesive films were employed to elevate the adhesion between the CFRP laminates, and SMA (NiTi) foils [94, 95]. Laser shot penning methodology was also used to enhance the interfacial properties by improving the interfacial bonding [96]. Also, clearing the elliptic patterns from the SMA ribbon inserted in a glass fiber composite can significantly improve the adhesion and damping response [97]. Many researchers also focused their research on improving the interfacial strength by creating micro-geometries and depositing nails on the surface of the SMA [98]. Nails on the surface displayed a 36% improvement in the interfacial resistance. SMA wire-embedded glass fiber reinforced composites were developed [91] and found to have improved bond strength after treating the SMA with acid and nano-silica particles. Touching upon other methods, a mechanical indentor was designed to create a uniform waviness pattern using knurled wheels on the surface of SMA wire, as shown in figure 9. Based on the wire pullout test performed on such indented SMA wires embedded in the vinyl-ester matrix, the interfacial bond strength is improved in comparison to a hand-sanded SMA wire composite by a factor of 5.21 and 8.58 for sparse and densely indented SMA wire composite, respectively [21].

H. Fathi *et al* [99] analytically and experimentally examined the stress distribution along the interface using the

minimum complementary energy principle in a two-cylinder model. It was concluded that a high value of pre-strain in SMA wire delays the debonding due to induced recovery stress. Additionally, the authors [100] also studied interfacial properties of SMA/epoxy composite at various crosshead speeds in a pullout and tensile test. The results indicated that a high loading rate reduced the tensile strength but elevated the interfacial shear strength. Zhang and Mi [101] explored the coating of SMA wire with nano-silica particles after being immersed in nitric acid for 8 hours. This method improved the interfacial bonding in NiTi SMA fiber-reinforced polymer composites by reducing the crack propagation due to coupling among nano-silica particles, SMA rough surface, and matrix.

4.1.4. Arrangement of SMA in the composite and size of the SMA.

1. **Location of SMA in the composite**: SMA location in the composite has been effective in achieving a specific output, such as shape change in the longitudinal or transverse direction, as shown in figure 10. SMAs are placed along the neutral axis or symmetrically in the cross-section of the plate to achieve active property tuning. The contraction of SMA applies a compressive recovery force over the entire cross-section in a dynamic situation [102]. The offset location of SMA develops a bending moment that can be utilized to impart shape morphing characteristics to SMAHC structures. This type of ASET is required for active shape control (ASC). Sun *et al* [103] analyzed the low-velocity impact on a laminated composite plate with SMA wires embedded in the top and bottom lamina. It was observed that an impact away from plate boundaries has better resistance to deformation due to the dominant super-elastic effect as compared to an impact near the edges.
2. **Size of the SMA wire**: SMA wire diameter for reinforcing into a composite is very crucial to apply recovery forces and transmitting the same to the matrix. The SMA wire with a large diameter will apply a very high amount of recovery force, which can be a cause of the interfacial failure and can damage the matrix. The thin SMA wire will not be able to provide a substantial amount of recovery force, which can be transmitted to the matrix material. Thin wires provide more surface area in comparison to large diameter wires for adhesion within the matrix. Sharma [62] optimized the wire diameter that can supply the required compressive force during the healing process in the composite structure. The objective was to achieve a minimal mass of SMA wires without any effect on the resistive heating. It was concluded that the 100 μm diameter wire causes a minimum weight increase. However, now there is a trade-off that a number of smaller diameter wires are required that can result in a considerable weight penalty.
3. **Orientation of the SMA wire**: The orientation of SMA wires determine the direction of recovery forces applied within the composite. It makes the structure direction-dependent. The direction of the SMA wire is highly sensitive to shape control applications. Zaman *et al* [104] investigated the effect of the orientation of SMA on the composite. The direction of the compressive force applied by SMA transformed by changing the orientation of SMA. This affected the stiffness other than the SMA along the fiber. The natural frequency of the sample reduced with 45° SMA fiber orientation, but the damping ratio increased in comparison to the sample with 0° SMA fiber orientation as shown in figure 11. Jang *et al* [105] investigated the effect of the orientation of SMA fiber for improving the strength of the SMA composite. They studied the effect stacking of CFRP layers at angles (0°, 30°, 60°, and 90°) of CFRP/NiTiNOL composites for fracture behavior. In contrast, a specimen with high stacking angles failed mainly by matrix cracking.

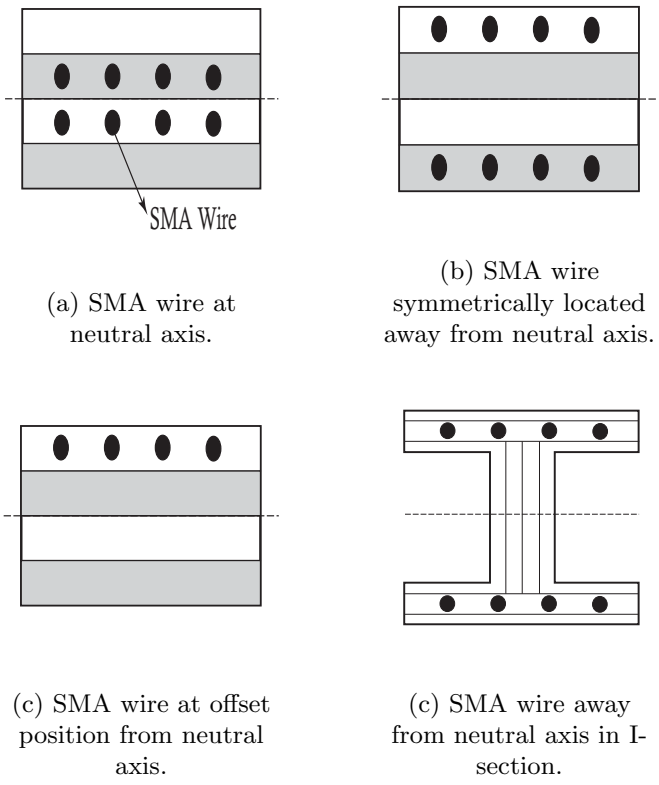

(a) SMA wire at neutral axis.

(b) SMA wire symmetrically located away from neutral axis.

(c) SMA wire at offset position from neutral axis.

(c) SMA wire away from neutral axis in I-section.

Figure 10. Schematic representations of SMA wire locations in the cross-section of a laminated composite.

4.1.5. Fatigue behavior of SMA-reinforced polymer composite.

Shape memory alloys endure through numerous cycles of thermo-mechanical deformation that ultimately causes fatigue failure. Such an event often occurs due to fracture under the cyclic stress-strain at constant temperature and thermal hysteresis, leading to degradation of SME and super-elasticity [106].

In addition, SMA composites are also employed to compensate for the fatigue of other structures. The SMA reinforcement in thermosetting matrix composites is desired due to their high impact absorption, corrosion resistance, high strain recovery, and damping capacity. The patches of such fiber-reinforced polymer (FRP) can also be retrofitted to

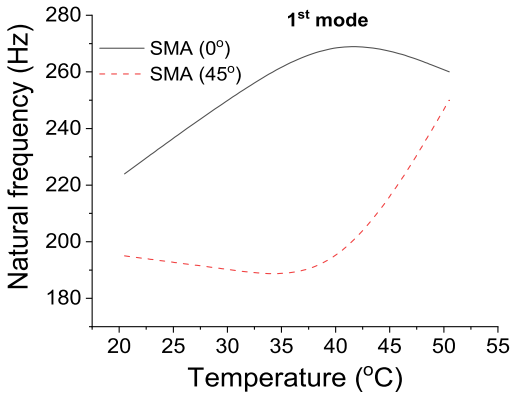

(a) Variation of the first mode of vibration.

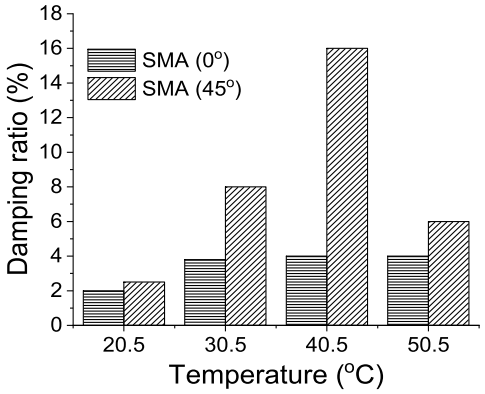

(b) Variation of damping ratio.

Figure 11. Composite GFRP with SMA in longitudinal direction 0° and at 45° [104].

bridge the fatigue cracks in engineering structures [107–110]. B. Zheng *et al* [111] prepared thermally activated SMA/CFRP composite patches that can be bonded to crack-sensitive regions of the steel structure substrate for extended fatigue life. The SMA wires constraints the crack path by applying compressive stress, and CFRP minimizes the stress contour around the crack by offering additional stiffness. This integration enhanced fatigue life by 26 times under sinusoidal loading. Z. Wang *et al* [33] investigated the fatigue behavior of SMA/glass-fibre/epoxy composite using a tapered sinusoidal signal as the fatigue cycle. It has been observed that fatigue life almost doubled due to the incorporation of superelastic SMA wire in comparison to only glass-fiber/epoxy composites. Thus, SMA wires are efficacious in improving fatigue performance by resisting the cracking of matrix and inhibiting the growth of the crack. Further, the scanning electron microscopy (SEM) images revealed the similarity in the mode of failure under the fatigue and static load. The fatigue failure mode includes crack in the matrix, delamination, breakage of fibers, shear failure of SMA-matrix bond, and the pull-out of SMA wires.

4.2. Fabrication

Continuous SMA composites can be fabricated using conventional hand-lay-up techniques while using the pseudoelastic SMA wires. However, this is not possible with the use of active pre-strained SMA. The embedded continuous SMA recovers its pre-strained shape while curing. Special arrangements are required to be designed for fixing the SMAs at the end to avoid the recovery of pre-strained SMA wire. The vacuum bagging can also be considered in addition to the hand lay-up technique. Initially, SMA composites were developed by mechanically fixing the SMA on surfaces of elastic beams for active vibration control [112]. Baz *et al* [113] reinforced SMA using sleeves in a flexible beam to regulate the buckling and vibration response. Residual stresses were developed during the curing process. Turner [114] used SMA ribbons for the fabrication of the glass fiber composite. Reverse transformation during the high temperature curing cycle was controlled by designing a mechanical frame [115].

Xu *et al* [116] used SMA of a very high actuation temperature above the processing temperature to avoid the clamping of SMA. A blocking system for SMA wire was avoided by using polyester resin with a low curing temperature than the austenite finish temperature [117]. Kirkby *et al* [118] developed a post-cure schedule that eliminated the need for a frame. A frame was developed by Zhou *et al* [79] to ensure alignment of SMA wires and desired spacing among the pre-strained wires. Behrooz *et al* [119] designed a system using a rigid steel frame consisting of adjustable and fixed rods that allows us to pre-strain the SMA wire and successfully integrate them between the composite laminates. SMA wire embedded glass fiber reinforced composites were also developed using vacuum-assisted resin injection processing and cured at room temperature with a vacuum level of 600 mbar for 24 hr. [91]. The interfacial microstructure was strong enough to bear the maximum activation stress. This level of vacuum and room temperature curing has produced good interfacial bonding. However, there are manufacturing difficulties and problems associated with the development of residual stresses. A well-designed post-cure cycle can avoid the reverse transformation situation and eliminate the need for a frame.

4.3. Applications

4.3.1. Shape control. This is a very promising area of continuous SMA application due to the high recovery force and high contraction during phase change. There are many applications of shape control that can be found in space structure, space antenna reflectors, and aerofoils shape morphing for aerospace applications. Shape change of polymer composite based structure with a good amount of force is required for soft robotics applications as in the case of grippers. The large volume fraction of continuous SMA is required to produce a good amount of recovery force [120]. Soft morphing is also an emerging technology for mimicking the compliant motion. Sometimes the target is to achieve the desired shape, while in other cases, it can be used for the control of buckling. The continuous embedded system is beneficial for changing the

shape of the structure without compromising the structural stiffness [112]. Some experiments were done on elastomeric cylinders with pre-strained SMA wires embedded eccentrically [121]. Paine *et al* [122] designed a cylinder of the polymer matrix composite with an SMA composite layer outside the cylinder. The pre-strained SMA generated recovery stress to produce external pressure on the inner layer of the cylinder to reduce the radial expansion or reduce the peak hoop stress. The durability of SMA embedded structures used for shape control has been an issue for research [123]. Degradation in terms of interfacial de-cohesion in these hybrid composites starts due to cyclic actuation. Active shape control of structure for pointing accuracy with the use of embedded SMA was discussed by Song *et al* [124]. The tip of the beam was moved to reach 7 mm deflection in 25 seconds with a robust compensator. Ryu *et al* [63] simulated the deformation behavior of the SMA-embedded GFRPs composite. Silicon rubber was added into a matrix of the GFRP composite as more compliant material. The simulation was performed to analyze the essential parameters required to realize the favorable stiffness and deformation of the structure. A single SMA wire embedded into PMC can conveniently generate bending deformation. However, to attain a complex motion of bend-twist nature, a different SMA actuator is required to produce multiple radii of curvature by modifying the stiffness of the material. Song *et al* [125] realized complex motion and shape control with a scaffold structure with four different modes of motion and shape control. A reversible bending response from an initially flat configuration to 90° angle was developed, and it was regulated by the local thermal activation of the shape memory polymer while it transforms from glassy to the rubbery state by the resistive heating of SMA actuators [126]. The SMA-reinforced glass fiber polymer composite has been studied for designing the active movement of the inchworm robot [127].

4.3.2. Stiffness modification. Continuous SMA wires or ribbons are also the source of modifying the stiffness of the polymer matrix composite due to residual stresses and high actuation stresses of SMA. During curing, polymer matrix composites are heated above the austenite finish temperature to transform detwinned martensite into the austenitic phase. SMA contracts and acts against the constrained matrix. Residual stresses are developed as a result of high contrast in the thermal expansion coefficients of the SMA and the matrix. Residual and constrained recovery stresses developed in the matrix improves the yield strength of the composite. Reinforcing composites with negative thermal expansion coefficient fibers [128], such as Kevlar and carbon fibers, are effective in increasing the reliability of the interface. SMA wires can be embedded around the outer surface of rotating drive shafts to adjust the bending stiffness of a rotating beam [129].

4.3.3. Vibration control. Controlling the vibrations using SMA is the first application of SMA in composite structures [112, 130]. Generally, superelastic SMA is used for controlling vibration due to the hysteresis effect. SMA composite design parameters have a strong influence on the specific damping capacity (SDC) and vibrational modes of SMA hybrid composite structures [131]. Controlling vibrations by shifting of natural frequency can be managed by altering the stiffness of the structure. The martensitic transformation is ideally a thermo-elastic transformation. However, various irreversible processes dissipate energy through crystal imperfection and dislocation movements. The development of the austenite-martensite interface produces defects and is a major source of thermo-mechanical coupling, while the austenite phase has poor intrinsic damping. Vibration control in active and passive modes are described here as below:

1. **Active vibration control**: An active method of vibration control deals with controlling vibration using parameters that can be controlled by external systems. Here, the heating of SMA by resistive heating or by externally heated environments is the externally controlled parameter. Natural frequency is a function of the stiffness of the material. Stiffness of the SMA increases as the temperature reaches above austenite finish temperature, and the low modulus martensite phase transforms into a high modulus austenite phase. Hence, stiffness and natural frequency of SMA composite increases in active mode. This technique is covered under active property tuning (APT), which is used to shift the natural frequency [38]. The natural frequency can be further modified by embedding pre-strained SMAs into the composite. Lau *et al* [130] embedded 0.5 mm Nitinol SMA into a balanced (0°/90°) glass-fiber epoxy beam of size 200 mm× 25 mm× 1.5 mm. It was observed that with an increase in SMA wires, the natural frequency did not improve significantly, but the damping ratio heightened in the dual-phase situation. So, the transition phase occurs during phase transformation from martensite to austenite or vice versa. Further, in the case of the actuation of the pre-strained SMA wires, and induced high tensile stress elevated the natural frequency of glass and carbon fiber (relatively higher modulus) composite beams by 6.9% and 2.09%, respectively added with good damping behavior as shown in figure 12.
   In low amplitude vibrations, the frequencies and amplitudes are a function of the recovery stress and stiffness. These are modified by tuning the recovery stress through SMA heating. Bidaux *et al* [132, 133] investigated the vibrational properties of the polymer/epoxy composite embedded with 1% volume NiTi fibers with 5% pre-strain. The natural frequencies updated by up to 50%.
   Rogers *et al* [4] experimented on the graphite-epoxy composite for structural acoustic control of the hybrid composite structure. Subsonic structural-acoustic radiation was controlled in a clamped beam of 82.2 cm× 2.03 cm× 0.01 cm graphite-epoxy-SMA hybrid composite. Malekzadeh *et al* [134] analyzed the free vibration behavior of 8 layers $(0/90/90/0)_s$ of graphite-epoxy SMA plate. Natural frequencies were higher when the pre-strain of wire, volume fraction and temperature were escalated. Schetky *et al* [135] found the significant effect of active SMA in composites for boundary conditions. Epps and Chandra [136] studied the role of embedding the SMA into

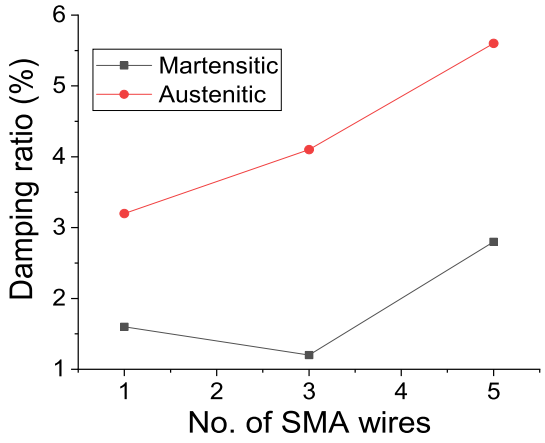

(a) Damping ratio with different number of non-prestrained embedded SMA wires into the composite beam.

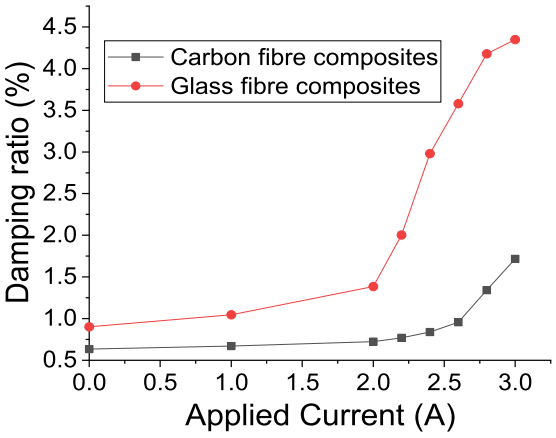

(b) Variation of damping ratio of two pre-strained embedded SMA wires into the composite beams at different applied currents.

Figure 12. Variation of damping ratio in the SMA-embedded composite [130].

graphite/epoxy beams using sleeves. SMAs were fixed at the ends of the sleeves and activated by resistive heating. A significant increase of 22 % in the first natural frequency was observed by embedding the 2% volume fraction of wires of SMA. An increase of 23% in the fundamental frequency of an actual helicopter composite shaft was also observed with embedding less than 8% volume fraction of SMA. Sittner *et al* [115] investigated the NiTiCu SMA to shift the natural frequency from 360 Hz at room temperature to 450 Hz at 100°C of Kevlar/epoxy with SMA.

2. **Passive vibration control**: This technique is employed to control the vibration without regulating the parameters by an external power. This may be achieved by using the hysteretic effect of superelastic SMA when externally applied stress is above the critical stress. Hysteretic loops with an extensive area of loop produce high inherent material damping. High material damping is required for polymer composite structures to avoid composite failure under vibrations. Design parameters of SMA composites such as volume fraction of constituent materials and interface characteristics affect the damping of SMA composites. Damping characteristics of pseudoelastic SMA-embedded glass fiber composite beams was studied and compared with steel wire embedded in the replacement of SMA by Gupta *et al* [137]. Damping ratio enhancement was two times the damping of steel wire embedded GFRP.

4.3.4. Damage suppression. The continuous form of SMA can be used for suppressing the impact damage by improving the fracture toughness of hybrid polymer composites. SMAs stores and dissipate the strain energy through the combination of stress-induced martensite transformation and plastic yielding. This kind of strain energy dissipation is immense as compared to high alloy steel and more than ten times of many graphite/epoxy composites. The superelastic or stress-induced martensite phase transformations are used for the impact damage suppression mechanism in passive mode. The damage suppression mechanism of the SMAHC consists of continuous SMA wires with SME effect, which helps to absorb and dissipate the impact energy. Rogers *et al* [12] discussed the method to extend the life of material by restricting the crack propagation by producing contraction forces using continuous SMA [138]. Saeedi and Shokrieh [139] experimentally studied the effect of pre-strained SMA for improving fracture behavior of the polymer. The crack growth resistance of 67% was observed with a 1% pre-strained SMA. Further, in comparison, there was a significant improvement in resistance to crack growth of epoxy by 2 and 4 times with 2% and 4% pre-strained SMA, respectively. Embedding the SMA NiTiNOL wires transverse to the crack and using shape memory effect to create compressive forces for closing the crack, also assists in curing [107]. Pappada *et al* [77] investigated the role of NiTiNOL wires for damage initiation sites in carbon and glass fiber composites. The dissipation of impact energy in carbon fiber-reinforced polymer composites with pseudoelastic NiTi wire was measured at different impact loads and observed the 100% dissipation of highest impact energy [78]. The SMA fiber reinforced hybrid composite patches were investigated [84] for repairing and found to deliver improved performance. Polymer matrix crack healing using the shape memory effect of SMA was simulated using a variational asymptotic approach [62]. The recovery force of SMA was able to heal the crack due to the softening of the polymer matrix above the SMA austenite finish temperature. The SMA/CFRP patch was investigated to repair a cracked steel structure and for improving the fatigue life [140].

4.3.5. Self-healing. Since most of the engineering structures are nature-inspired, biological systems are most insightful. An essential characteristic of living entities is self-healing,

and the same is also desired from engineering materials for enduring life. The assimilation of self-healing ability in materials assists in closing the micro-cracks autonomously. Over the past few years, through various studies, the application of SMA reinforcements in composites has been investigated rigorously to bio-mimic the phenomenon of self-healing [141–143]. A detailed comparative analysis of various mechanisms of self-healing, such as capsule-based and vascular healing, are summarized by Y. Wang *et al* [144]. The basic idea of embedding SMA for self-healing is to employ the superelastic and shape memory effect for improving the fracture behavior of composites by crack pre-closure [145]. Also, the dynamic impact damage suppression capabilities of SMA are beneficial for designing self-healing composites [146].

Kirkby *et al* [141] explored the self-healing process of a pre-strained SMA/epoxy-based composite consisting of microcapsules enclosing a healing agent (dicyclopentadiene) and a catalyst. Self-healing was assessed by computing the peak load that induces a fracture after healing in a tapered double cantilever beam (TDCB) sample. The results support the claim by authors during the previous study of injecting the healing agent manually [147]. It was observed that the peak load after healing was estimated to be around 80% of the peak load in the original sample. Besides, due to the presence of embedded SMA wires, a lower quantity of the healing agent was sufficient to impart desired healing. The SMA wires provided the closure force that minimized the crack volume and heating effect of SMA assisted in enhancing the cross-linking during the polymerization.

Saeedi *et al* [148] examined the effect of 2% pre-strained superelastic embedded SMA wires on the fracture toughness of the epoxy polymer using double cleavage drilled compression tests. It was established that fracture toughness improved by 15%. However, a rise in pre-strain value weakened the SMA-matrix bond and degraded the mechanical properties. The self-healing efficiency of the thermally reversible polymer was investigated using the SME effect with a 2% pre-strained SMA. A healing efficiency of 92% was obtained against the value of 43% for specimens without SMA wire.

4.3.6. Health monitoring. The continuous form of SMA is used for the health monitoring of composites with the help of sensing characteristics like other smart materials such as piezo-ceramic and PVDF. These sensing parameters are directly or indirectly for assessing the health of the polymer composite structures. The application of SMA as a sensor is based on the change in the material property due to phase transformation. Cui *et al* [149] explored the association between strain and electrical resistance variation in an SMA to investigate the sensing characteristics of such material. These specific features are measured to access the damages in the composites. Nagai *et al* [150] demonstrated that the amount of damage in a hybridized GFRP could be evaluated via monitoring the electrical resistance variations of the embedded SMA. Generally, pseudoelastic SMA is used for sensing. Sometimes, change in the resistance is measured as a function of integrated strain. The high resistivity of NiTiNOL befits it to be used as a sensor with the support of the Wheatstone bridge. NiTiNOL can be used as a dual-mode sensor because it can sense temperature as well as strain. Embedding sensors such as optical fiber into the composite can cause premature failure. One of the design requirements for an intelligent composite structure is to use reinforcements as a sensor as well as an enhancer of the structural property of the composite. These types of systems are referred to as a self-sensing system. The sensor is an integral part of the composite.

Resistance-based self-sensing can be used for damage detection and to trace the location of the damage. Health monitoring requires both quantification and location of damages. The plotting of conductivity values over a domain can clearly show the location of the damage. SMA wires have been used as strain sensors with low transformation temperature (-30°C to $+10^{\circ}$C) [151]. The design of such adaptive hybrid composites with self-sensing lamina endeavor a high gauge factor in comparison to conventional strain gauges. An effort was directed to monitor the resistance based on damage locations using pseudoelastic wires in a glass fiber polymer composite [152]. Pinto *et al* [153] used the thermography method to detect damage from impact or other dynamic loadings in SMA composites. Embedding iron-based magnetic SMA (MSMA) wires provides the capability of monitoring structural health using external magnetic field sensing. Localized phase change occurs in MSMA wire at damage locations. These phase changed locations modify the magnetic field lines passing through the damaged locations. The magnetic field line helps to detect the damages [154].

5. Discontinuous SMA composites

An array of SMA-based hybrid composites (SMAHCs) are feasible with the use of discontinuous SMA as small sections of wire/ribbons, and in the form of particulates with various aspect ratios. Continuous SMA fibers impart directional properties, whereas the short randomly oriented fibers deliver isotropic properties. Fabrication of a continuous SMA-based composite is arduous in comparison to the discontinuous SMAs that offer the advantage of dispersing the residual stress over the polymer matrix. Interfacial failure is also not an issue in discontinuous-based composites. Detailed discussions of composite design, fabrication, essential factors affecting the performance and applications are considered in the following sections.

5.1. Design parameters

The design of discontinuous SMA-based composite is primarily dependent upon the properties of matrix and SMA, the aspect ratio of SMA short fibers, and their volume fractions. Sleeves are not mandatory for embedding short SMA wires as they remain intact within the matrix. Such composites have a basic mechanism for modifying the properties similar to conventional short fibers composites; additionally, they can be controlled passively or actively. In the passive applications, the pseudoelastic SMA short fibers are incorporated to heighten

the strength of polymer matrix composites, store strain energy, and increase the residual stresses. While the active applications offer to tune stiffness, natural frequency, and damping of SMA composites.

5.1.1. Effects of the constraining matrix. In short-fiber embedded polymer composites, the matrix is constrained, and the fibers are loaded indirectly through the matrix. Therefore, matrix properties and interfacial bonding are essential for the performance of short fiber-based polymer matrix composites. Short fiber inside the matrix actuates under a suitable thermal environment and tries to apply stresses into the matrix. These stresses change the energy balance of the matrix system. The bonding at the SMA wire/polymer matrix interface must be adequate to transfer stresses to the surrounding material medium. Thus, the composite exhibits excellent damping properties due to the interfacial interaction of fiber with the matrix system. As a result, discontinuous SMA composites have a higher potential for improving the damping properties of polymer composites due to the actuation of SMA for dampening and shape control [155].

5.1.2. Effects of pre-strain and volume fraction. Similar to continuous SMA elements/wires, the pre-strain level of short SMA determines the amount of recovery stress. Contraction of short SMAs produces compressive residual stresses into the matrix, which increases proportionally to the volume fraction [52]. Zhang *et al* [156] found that the addition of optimum weight fraction from 0% to 3.5% of discontinuous SMA fillers into the epoxy matrix elevated the storage modulus and residual thermal stress with the increase in filler weight percentage. Beyond this optimum value, both get reduced. Fracture deflection decreased due to brittle failure with the increase of SMA volume fraction. The loss factor escalated with the increasing amount of discontinuous filler content. Lei *et al* [157] concluded that the storage modulus is primarily affected by the volume fraction of SMA as a change in temperature, induced by the change in stiffness or elastic modulus.

5.1.3. Interfacial bonding. The performance of short SMA polymer composites structure is dependent on the SMA-polymer matrix interfacial bond. In an active state, an optimum interfacial bonding is responsible for transferring the maximum load applied by the pre-strained SMA. The stiffness of the surrounding matrix also affects the properties of the composite. A high shear force is induced in a stiffer polymer matrix, significantly improving the dynamic response. The interaction of short SMA fiber within the matrix affects the generation of recovery stress. Lei *et al* [158] investigated the interface between the superelastic short SMA fiber and matrix on the overall mechanical behavior of composites. It was observed that the interfacial separation increases with the increase of loading time. The rise in temperature from 320 K to 360 K did not alter the fiber-matrix interface friction, maximum yield stress, and strain in a composite.

5.1.4. Arrangement of discontinuous SMA into composites and aspect ratio.

1. **Location of SMA into composites**: The discontinuous SMAs are randomly distributed into the polymer matrix to provide an isotropic effect or embedded into the specific layer at/around the neutral axis, symmetrically in layers away from the axis. The location of the SMA in the composite structure is governed by the mechanism of response adopted. The response of discontinuous SMAs is similar to the continuous SMAs embedded composites according to the location of the SMA embedded layer.
2. **Aspect ratio**: Lei *et al* [158] concluded that the size of discontinuous SMA is a key factor in determining the overall response of the composites. In the case of short fibers, a geometrical quantity related to size is the aspect ratio. The effect of lowering the aspect ratio reduced the overall Young's modulus of the composite. Murasawa *et al* [52] concluded that the short and long wires have a very comparable response for an aspect ratio greater than 25.

5.2. Fabrication

The discontinuous SMA composites with polymer matrix can be easily fabricated by mixing discontinuous SMA into the polymer matrix and then pouring the mixture into a mold for curing. Discontinuous SMA-reinforced fiber polymer matrix composites are fabricated by the hand-lay-up technique by embedding the SMA into a specific layer of composites. Small diameter (0.1–0.150 mm) wires are suitable for embedding between the layers. The injection molding technique can fabricate discontinuous SMA-based thermoplastic matrix composites. Murasawa *et al* [159] fabricated the short SMA fiber-embedded composites with the injection polycarbonate matrix and using an injection molding machine. The ferromagnetic SMA (FSMA) magnetic particle can also be embedded into the polymer matrix composite by fusing with the hand lay-up method. The discontinuous FSMA can be aligned by applying mechanical stress in the desired direction to form the easy axis magnetization. The particles or short fibers are aligned with the help of curing under the magnetic field.

5.3. Applications

5.3.1. Shape control. Discontinuous SMAs have been rarely used for the control of polymer matrix-based structures. Shape control of polymer composites has not been investigated for controlling the shape of structures. SMA particulates were embedded into the grooves with a silicon matrix [160].

5.3.2. Stiffness modifications. Super-elastic SMAs are used for passive application with discontinuous SMA embedded into the polymer composite. The modulus of elasticity of the austenite phase is very high in comparison to the martensite phase. So, the strength and stiffness of the polymer composite can be improved with this high modulus phase of austenite into the polymer composite. This increases the applicability

of the polymer composite for dynamic load applications. The short fiber SMA-reinforced composite displays the low fracture strain in comparison to large strain in continuous SMA fiber-reinforced composites [52, 159]. The effect of fiber on the deformation behavior of short-fiber reinforced was not remarkable. The tensile properties [161] and bending properties of short fiber-reinforced epoxy composites were evaluated [162]. Pre-strained particles are also used to increase the effectiveness of each particle in the polymer composite following the similar mechanism of pre-strained continuous SMA fibers into the composites. The pre-strained randomly oriented SMA particles recover their shape, and compressive stresses are induced into the matrix in all directions. Longitudinal strength and stiffness are not much affected by the SMA particles. The stress-induced transformations of spheroidal particles have a significant effect in escalating the bending strength and stiffness of composite, even in the presence of low SMA volume fraction [160]. This result suggested that the SMA particle composite displayed brittle fracture behavior.

5.3.3. Passive and active vibration control. The natural frequency of the polymer composite increases with reinforcement of high modulus superelastic SMA. Thus, it shifts the resonance frequency away from the operational frequency. Some of the properties of the short SMA composite are modified using a similar mechanism of the long SMA fiber composite in active mode. Compressive stresses are generated while recovering its shape during the reverse transformation. Reverse transformation improves the tensile strength of the composite. Khalili *et al* [163] performed the experiments to evaluate the static and dynamic properties of SMA short wires reinforced resin. Murasawa *et al* [159] studied the effect of the interface, fiber volume fraction, and aspect ratio on the generation of internal stress in the polycarbonate matrix. Increasing the volume fraction of short SMA from 5% to 30%, the composite strain reduces and becomes negative during phase change from 60°C to 90°C. At this volume fraction of short SMA, the composite developed strain similar to a long fiber composite. Due to SME, the residual stresses in the fiber and matrix are opposite, and the strain history is different for long and short fiber composite during heating, as illustrated in figure 13 [52].

The effect of aspect ratio was not significant on residual stresses, deformation, and generation of internal stresses. The performance of short SMA reinforced composite was similar to continuous SMA reinforced composite with high aspect ratio and volume fraction of SMA. Zhang *et al* [70] investigated the role of dispersing discontinuous forms of SMA into the epoxy resin. An increase in storage modulus and loss factor was observed with SMA fillers. The loss factor of polymer composites embedded with SMA particle fillers is found to be higher than the polymer composite with SMA short fiber fillers. Next, the ferromagnetic SMA (FSMA) magnetic particles of Ni-Mn-Ga were embedded in an aligned manner into the polymer matrix composite [164]. The role of aligned particles was explored due to the presence of twin boundaries. The damping of the composite escalated due to twin boundaries.

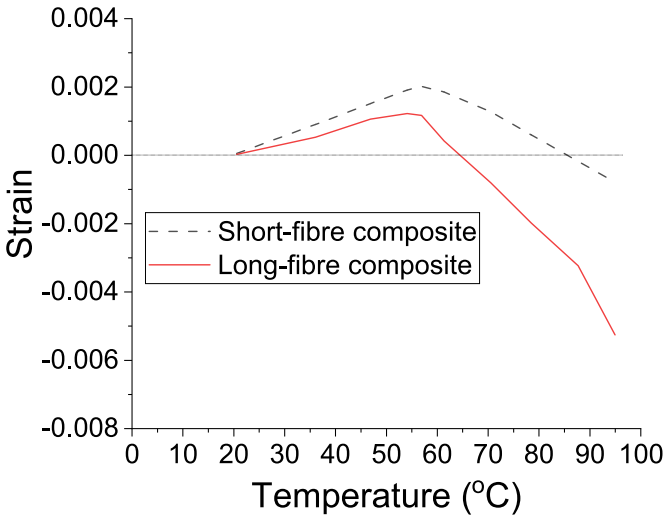

Figure 13. Behavior of short and long SMA composites under the heating process [52].

5.3.4. Damage suppression. The status of damage suppression capabilities of short SMA composite can be predicted from a general class of short fiber-based composites. The damage is initiated at the interfaces, and shear strength is also reduced. So, it is clear that damage suppression capability is not expected in this type of composite. The healing of the interfacial adhesion can potentially recover the stiffness of short-fiber SMA composites.

5.3.5. Health monitoring. The SMA particles embedded in the structure can be availed for health monitoring of the structure with the help of stress-induced phase transformation behavior. The health of the structure can be accessed by observing the changes in mechanical and electromagnetic behavior of discontinuous forms of SMA when a crack is generated in the vicinity of these discontinuous SMAs [165].

6. Challenges with SMA-based polymer composites

SMA-embedded polymer composites have many potential and embryonic applications. However, some certain ingrained limitations and challenges seek immediate attention.

6.1. Optimal design

Promoting the use of polymers matrix-based SMA composites over conventional polymer matrix-based composites demands a considerable technology leap as interfacial bonding between matrix and SMA determines the performance of the SM- embedded composites. An optimized level of interfacial bonding is thus fundamental for operation. Rigid bonding restricts the actuation capabilities (SME effect) of SMA, while being lax in interfacial bonding does not enable SMA to have adequate contact with the matrix under the applied load. Further, the proper SMA wire diameter should be selected given the availability of surface area per unit mass of SMA for adhesion and load transfer. Hence, it is challenging to

manage the factors responsible for interfacial bonding. One way to achieve this is by controlling the curing cycle of the thermoset matrix material. Besides, the matrix glass transition temperature should also be higher than the SMA transformation temperature.

In the case of thermoplastic matrix-based SMA composites, high processing temperature for the thermoplastic matrix shifts the transformation temperature of SMA and reduces the peak recovery stress [18]. Hence, finding suitable thermoplastic material having a lower glass transition temperature than SMA transformation temperature is also an additional obstacle.

There are many other arrays of design issues that significantly affect the properties of SMA composites, such as SMA volume fraction, orientation, and stacking sequence of SMA. Extensive experimental work is crucial to obtain the suitable values of each parameter for a specific application. The aspect ratio of particulate or chopped fibers of SMA is also a deciding factor in the case of discontinuous SMA composites.

SMA fibers are activated by resistive heating that produces a shape memory effect (SME). Active continuous SMA-based composites consist of wires extending out of the specimen, which provides the space for current supply. However, structural integrity gets compromised in this process. SMA absorbs energy during the entire transformation process, and the temperature increases. Usually, the polymer matrix is a poor conductor of heat; as a result, heat dissipation is difficult. Efforts should also be directed to increase the thermal conductivity of the matrix material. Mostly, discontinuous SMA-based composites are passive or are active under external thermal environment. It is quite challenging to manufacture active discontinuous SMA-based polymer composites with an internal heating source that eventually requires a matrix of relatively high electrical conductivity.

6.2. Fabrication

SMA-reinforced composites also have fabrication complications. Special fixtures are desired for holding the SMA wires and maintaining the pre-strain while preparing continuous SMA wire-based composites. The surface treatment of SMA fibers also plays an important role in interfacial strength. Identifying the suitable methodology for pre-treatment of SMA fibers such as acid etching, hand-sanded, sandblasted, and plasma coat is crucial. During fabrication, constraining the matrix elevates interfacial shear stress induced in the matrix. Hence, the constrained system makes the fabrication additionally cumbersome. Thus, it is a good design challenge to overcome this contradiction.

7. Conclusions

The state-of-the-art in shape memory alloy-reinforced polymer composites has been reviewed for shape control of structure and enhancement of static and dynamic properties of composites. Modeling for SMA, SMA-reinforced composites, and short SMA-reinforced composites are scrutinized in this direction. A special focus has been made on shape control, stiffness modification, vibrational control, damage suppression, self-healing, and health monitoring applications. The following conclusions have been drawn from the presented review:

1. A selection of matrix material in the form of polymer-only or polymer-based composite material should be decided considering the modulus of elasticity of the matrix material and desired application of SMA-embedded composites.
2. Interfacial bonding is key for managing tailored stiffness for providing required actuation capability.
3. The appropriate position of SMA wires inside the composite structure should be selected to attain the desired effect. For instance, the damping properties can be enhanced by inserting the SMAs inside the laminate. The shape morphing can be achieved by either controlling the plain strain (SMA wires at the neutral plane of the composite) or by regulating bending properties (SMA wires away from the neutral axis). To effectively close a crack, SMAs can be inserted through the reinforcement thickness as a continuous stitch.
4. Low processing temperature than the transformation temperature of SMA is required to make fabrication easy without the need for the special fixture.
5. Pseudoelastic SMA-based structures are easy to fabricate and can be used in comparison to SME effect-based structure.
6. Discontinuous SMAs are useful for improving material properties in the passive or active mode under the electric/magnetic field. In order to operate in the active mode using resistive heating, the entire matrix has to be electrically conductive. However, transformation temperature should not be very high in order to prevent degradation of the polymer matrix due to overheating.

Following research directions can be examined for future research in the domain of SMA-based polymer composites:

1. In general, soft/low stiffness polymers are incorporated for SMA-based shape control applications. Nevertheless, research work concerning the identification of fiber-reinforced polymeric composites with tailorable and optimized stiffness suitable for shape control applications with structural properties may be pursued.
2. A rigorous analysis of the curing cycle is required to predict active SMA properties for the thermoset polymer-based SMA composites.
3. The effect of discontinuous SMA on mechanical properties is required to be investigated for high strength fiber composites. There is a need for more focus on resistively heated discontinuous SMA composites.
4. Exploring the use of 3D printing over SMA wire mesh should be scrutinized.
5. Novel microstructure likes cellular composites integrated with SMA may be explored.

ORCID iDs

Arun Kumar Sharma https://orcid.org/0000-0002-2952-3177
Bishakh Bhattacharya https://orcid.org/0000-0002-9621-5246
Sondipon Adhikari https://orcid.org/0000-0003-4181-3457

References

[1] Wayman C M, Duerig T W 1990 *An Introduction to Martensite and Shape Memory* (Butterworth-Heinemann)
[2] Huber J E, Fleck N A and Ashby M F 1997 The selection of mechanical actuators based on performance indices *Phil. Trans. R. Soc.* A **453** 2185–205
[3] Huang W M, Ding Z, Wang C C, Wei J, Zhao Y and Purnawali H 2010 Shape memory materials *Mater. Today* **13** 54–61
[4] Rogers C A 1990 Active vibration and structural acoustic control of shape memory alloy hybrid composites: Experimental results *J. Acoust. Soc. Am.* **88** 2803–11
[5] Kakeshita T, Saburi T, Kindo K and Endo S 1997 Effect of Magnetic Field and Hydrostatic Pressure on Martensitic Transformation and Its Kinetics. Japanese *J. Appl. Phys.* **36** 7083–94
[6] Sozinov A, Likhachev A A, Lanska N and Ullakko K 2002 Giant magnetic-field-induced strain in NiMnGa seven-layered martensitic phase *Appl. Phys. Lett.* **80** 1746–8
[7] Chernenko V A, Besseghini S, Müllner P, Kostorz G, Schreuer J and Krupa M 2007 Ferromagnetic Shape Memory Materials: Underlying Physics and Practical Importance *Sensor Lett.* **5** 229–33
[8] Kakeshita T, Kuroiwa K, Shimizu K, Ikeda T, Yamagishi A and Date M 1993 A New Model Explainable for Both the Athermal and Isothermal Natures of Martensitic Transformations in Fe-Ni-Mn Alloys *Mater. Trans. JIM* **34** 423–8
[9] Fabrizio Q, Loredana S and Anna S E 2012 Shape memory epoxy foams for space applications *Mater. Lett.* **69** 20–3
[10] Xiong J Y, Li Y C, Wang X J, Hodgson P D and Wen C E 2008 Titanium–nickel shape memory alloy foams for bone tissue engineering *J. Mech. Behavior Biomed. Mater.* **1** 269–73 Biological Materials Science
[11] Gu Q, Van Humbeeck J, Delaey L, Federzoni L, Guénin G and Gex D 1995 Effect of Amount of Deformation on the Martensitic Transformation and Shape Memory Effect in Fe-Mn-Si based Shape Memory Steel *J. Phys. IV France* **05** 311–15
[12] Rogers C, Liang C and Jia J 1989 Behavior of shape memory alloy reinforced composite plates. I—Model formulations and control concepts *30th Structures, Structural Dynamics and Conf.* pp 2011–17
[13] Srivastava R, Sharma A K, Hait A K and Bhattacharya B 2018 Design and development of active bimorph structure for deployable space application editor Erturk A *Active and Passive Smart Structures and Integrated Systems XII* (Int Society for Optics and Photonics SPIE) pp 818–29
[14] Du X W, Sun G and Sun S S 2004 A study on the deflection of shape memory alloy (SMA) reinforced thermo-viscoelastic beam *Compos. Sci. Technol.* **64** 1375–81
[15] John S and Hariri M 2008 Effect of shape memory alloy actuation on the dynamic response of polymeric composite plates *Composites Part A: Applied Science and Manufacturing* **39** 769–76
[16] Jani J M, Leary M and Subic A 2017 Designing shape memory alloy linear actuators: A review *J. Intell. Mater. Syst. Struct.* **28** 1699–1718
[17] Kiesling T, Chaudhry Z, Paine J and Rogers C 1996 Impact failure modes of thin graphite epoxy composites embedded with superelastic nitinol *37th Structure, Structural Dynamics and Conf.* AIAA, Inc pp 1448–57
[18] Paine J S N, Rogers C A 1994 Improved impact damage resistance in adaptive shape memory alloy hybrid composite materials Hagood N W, editor *Smart Structures and Materials: Structures and Intelligent Systems* vol 2190 (Int. Society for Optics and Photonics. SPIE) pp 402–9
[19] Jang B K and Kishi T 2005 Thermomechanical response of TiNi fiber-impregnated CFRP composites *Mater. Lett.* **59** 2472–5
[20] Jang B K and Kishi T 2006 Mechanical properties of TiNi fiber impregnated CFRP composites *Mater. Lett.* **60** 518–21
[21] Yuan G, Bai Y, Jia Z, Hui D and tak Lau K 2016 Enhancement of interfacial bonding strength of SMA smart composites by using mechanical indented method *Compos. B: Eng.* **106** 99–106
[22] Jani J M, Leary M, Subic A and Gibson M A 2014 A review of shape memory alloy research, applications and opportunities *Mater. Des.* **56** 1078–113
[23] Barbarino S, Flores E I S, Ajaj R M, Dayyani I and Friswell M I 2014 A review on shape memory alloys with applications to morphing aircraft *Smart Mater. Struct.* **23** 063001
[24] Cohades A and Michaud V 2018 Shape memory alloys in fibre-reinforced polymer composites *Adv. Indus. Eng. Polym. Res.* **1** 66–81
[25] Pirondi A, Gandhi Y and Collini L 2019 Strategies for modelling and optimization of bi-stable composite laminates actuated by embedded Shape Memory Alloy wires. Procedia Structural Integrity *AIAS 2019 Int. Conf. on Stress Analysis* vol 24 pp 455–69
[26] Zhao P, Chen H, Li B, Tian H, Lai D and Gao Y 2019 Stretchable electrochromic devices enabled via shape memory alloy composites (SMAC) for dynamic camouflage *Opt. Mater.* **94** 378–86
[27] Quade D, Jana S and McCorkle L 2019 The influence of thin film adhesives in pullout tests between nickel–titanium shape memory alloy and carbon fiber reinforced polymer matrix composites *Compos. B: Eng.* **176** 107321
[28] Kapuria S and Das H N 2018 Improving hydrodynamic efficiency of composite marine propellers in off-design conditions using shape memory alloy composite actuators *Ocean Eng.* **168** 185–203
[29] Katsiropoulos C V, Pappas P, Koutroumanis N, Kokkinos A and Galiotis C 2020 Improving the damping behavior of fiber-reinforced polymer composites with embedded superelastic shape memory alloys (SMA) *Smart Mater. Struct.* **29** 025006
[30] Dahnke C, Pottmeyer F, Pinter P, Weidenmann K A and Tekkaya A E 2019 Influence of SMA-induced stress on shape memory alloy metal matrix composites manufactured by continuous composite extrusion *Smart Mater. Struct.* **28** 084006
[31] Mizzi L, Spaggiari A and Dragoni E 2019 Design-oriented modelling of composite actuators with embedded shape memory alloy *Compos. Struct.* **213** 37–46
[32] Akbari T and Khalili S M R 2019 Numerical simulation of buckling behavior of thin walled composite shells with embedded shape memory alloy wires *Thin-Walled Struct.* **143** 106193
[33] Wang Z, Xu L, Sun X, Shi M and Liu J 2017 Fatigue behavior of glass-fiber-reinforced epoxy composites embedded with shape memory alloy wires *Compos. Struct.* **178** 311–19

[34] Srivastava V and Gupta M 2019 Experimental assessment of self-healing characteristics in AA2014matrix with nitinol wire and solder alloy as healing agents *Mater. Res. Express* **6** 085704

[35] Perkins J and Hodgson D 1990 The Two-Way Shape Memory Effect Duerig T W, Melton K N, Stöckel D and Wayman C M *Engineering Aspects of Shape Memory Alloys* (Butterworth-Heinemann) 195–206

[36] de Blonk B J and Lagoudas D C 1998 Actuation of elastomeric rods with embedded two-way shape memory alloy actuators *Smart Mater. Struct.* **7** 771–83

[37] Tanaka K 1986 A Thermomechanical Sketch of Shape Memory Effect: One-Dimensional Tensile Behavior *Res. Mech.* **18** 251–63

[38] Liang C and Rogers C A 1990 One-Dimensional Thermomechanical Constitutive Relations for Shape Memory Materials *J. Intell. Mater. Syst. Struct.* **1** 207–34

[39] Brinson L C 1993 One-Dimensional Constitutive Behavior of Shape Memory Alloys: Thermomechanical Derivation with Non-Constant Material Functions and Redefined Martensite Internal Variable *J. Intell. Mater. Syst. Struct.* **4** 229–42

[40] Boyd J G and Lagoudas D C 1996 A thermodynamical constitutive model for shape memory materials Part I. The monolithic shape memory alloy *Int. J. Plast.* **12** 805–42

[41] Auricchio F, Taylor R L and Lubliner J 1997 Shape-memory alloys: macromodelling and numerical simulations of the superelastic behavior *Comput. Methods Appl. Mech. Eng.* **146** 281–312

[42] Auricchio F and Sacco E 1997 A Superelastic Shape-Memory-Alloy Beam Model *J. Intell. Mater. Syst. Struct.* **8** 489–501

[43] Bekker A and Brinson L C 1998 Phase diagram based description of the hysteresis behavior of shape memory alloys *Acta Mater.* **46** 3649–65

[44] Tanaka K 1990 A Phenomenological Description on Thermomechanical Behavior of Shape Memory Alloys *J. Pressure Vessel Technol.* **112** 158–63

[45] Sato Y and Tanaka K 1988 Estimation of energy-dissipation in alloys due to stress-induced martensitic transformation *Res. Mech.* **23** 381–93

[46] Ivshin Y and Pence T J 1994 A Thermomechanical Model for a One Variant Shape Memory Material *J. Intell. Mater. Syst. Struct.* **5** 455–73

[47] Auricchio F, Fugazza D and DesRoches R 2007 A 1D rate-dependent viscous constitutive model for superelastic shape-memory alloys: formulation and comparison with experimental data *Smart Mater. Struct.* **16** S39–S50

[48] Auricchio F, Marfia S and Sacco E 2003 Modelling of SMA materials: Training and two way memory effects *Comput. Struct.* **81** 2301–17

[49] Nallathambi A K, Doraiswamy S, Chandrasekar A S and Srinivasan S M 2009 A 3-species model for shape memory alloys *Int. J. Struct. Changes Solids* **1** 149–70

[50] Marfia S and Rizzoni R 2013 One-dimensional constitutive SMA model with two martensite variants: Analytical and numerical solutions *Eur. J. Mech. - A/Solids* **40** 166–85

[51] Sayyaadi H, Zakerzadeh M R and Salehi H 2012 A comparative analysis of some one-dimensional shape memory alloy constitutive models based on experimental tests *Sci. Iranica* **19** 249–57

[52] Murasawa G, Tohgo K and Ishii H 2005 The effect of fiber volume fraction and aspect ratio on the creation of internal stress in the matrix and deformation for short-fiber shape memory alloy composite *Smart Mater. Struct.* **15** 33–40 dec

[53] Lecce L and Concilio A 2014 *Shape Memory Alloy Engineering* (Butterworth-Heinemann)

[54] Kalra S, Bhattacharya B and Munjal B S 2017 Design of shape memory alloy actuated intelligent parabolic antenna for space applications *Smart Mater. Struct.* **26** 095015

[55] Rogers C A and Robertshaw H H 1988. Development of a Novel Smart Material *ASME Winter Annual Meeting, Chicago. vol. 88-WA/DE-9. ASME*

[56] Boyd J G and Lagoudas D C 1994 Thermomechanical Response of Shape Memory Composites *J. Intell. Mater. Syst. Struct.* **5** 333–46

[57] Sullivan B J 1994 Analysis of Properties of Fiber Composites with Shape Memory Alloy Constituents *J. Intell. Mater. Syst. Struct.* **5** 825–32

[58] Birman V 1997 Stability of functionally graded shape memory alloy sandwich panels *Smart Mater. Struct.* **6** 278–86

[59] Turner T L 2000 Thermomechanical response of shape memory alloy hybrid composites [PhD dissertation] Virginia Polytechnic Institute and State University (Available from: https://vtechworks.lib.vt.edu/handle/10919/29771)

[60] Ostachowicz W, Krawczuk M and Zak A 1998 Natural Frequencies of Multi-Layer Composite Plate with Embedded Shape Memory Alloy Wires *J. Intell. Mater. Syst. Struct.* **9** 232–7

[61] Balapgol B S, Bajoria K M and Kulkarni S A 2006 A two-dimensional finite element analysis of a shape memory alloy laminated composite plate *Smart Mater. Struct.* **15** 1009–20

[62] Sharma A K and Harursampath D K 2008 Variational Asymptotic Analysis of a Self-healing SMA Composite *Int. Conf. on Engineering Optimization* Rio de Janeiro, Brazil EngOpt 2008

[63] Ryu J, Jung B S, Kim M S, Kong J, Cho M and Ahn S H 2011 Numerical simulation of hybrid composite shape-memory alloy wire-embedded structures *J. Intell. Mater. Syst. Struct.* **22** 1941–8

[64] Cho H K and Rhee J 2012 Nonlinear finite element analysis of shape memory alloy (SMA) wire reinforced hybrid laminate composite shells *Int. J. Non-Linear Mech.* **47** 672–8

[65] Khalili S and Saeedi A 2018 Dynamic response of laminated composite beam reinforced with shape memory alloy wires subjected to low velocity impact of multiple masses *J. Compos. Mater.* **52** 1089–101

[66] Chang M, Kong F, Sun M and He J 2019 A Three-phase model characterizing the low-velocity impact response of sma-reinforced composites under a vibrating boundary condition *Materials* **12** 1

[67] Eshelby J D and Peierls R E 1957 The determination of the elastic field of an ellipsoidal inclusion and related problems *Proc. R. Soc. London Ser.* A **241** 376–96

[68] Wang J and Shen Y P 2000 Micromechanics of composites reinforced in the aligned SMA short fibers in uniform thermal fields *Smart Mater. Struct.* **9** 69–77

[69] Lei H S, Zhou B, Wang Z Q and Wang X Q 2012 Tensile Properties of Random Distribution Short SMA Fiber Reinforced Composites *Advances in Fracture and Damage Mechanics X. vol. 488 of Key Engineering Materials* Trans Tech Publications Ltd pp 686–9

[70] Zhang Y and Zhao Y P 2007 A study of composite beam with shape memory alloy arbitrarily embedded under thermal and mechanical loadings *Mater. Des.* **28** 1096–115

[71] Lei H, Wang Z, Zhou B, Tong L and Wang X 2012 Simulation and analysis of shape memory alloy fiber reinforced composite based on cohesive zone model *Mater. Des.* **40** 138–47

[72] Khalili S M R, Saeedi A and Fakhimi E 2016 Evaluation of the effective mechanical properties of shape memory wires/epoxy composites using representative volume element *J. Compos. Mater.* **50** 1761–70

[73] Khalili S M R and Saeedi A 2017 Determination of the elastic properties of randomly oriented shape memory alloy (SMA) discontinuous wires reinforced epoxy resin *Compos. Struct.* **180** 148–60

[74] Halpin J C and Kardos J L 1976 The Halpin-Tsai equations: A review *Polymer Eng. Sci.* **16** 344–52

[75] Biagiotti J, Fiori S, Torre L, López-Manchado M A and Kenny J M 2004 Mechanical properties of polypropylene matrix composites reinforced with natural fibers: A statistical approach *Polym. Compos.* **25** 26–36

[76] Jamian S, Mohamed N A N, Ihsan A K A M, Ismail A E, Nor M K M and Kamarudin K A *et al* 012016 Deflection of elastic beam with SMA wires eccentrically inserted *Conf. Series: Materials Science and Engineering* vol 2017 p 226:

[77] Pappada S, Rametta R, Toia L, Coda A, Fumagalli L and Maffezzoli A 2009 Embedding of Superelastic SMA Wires into Composite Structures: Evaluation of Impact Properties *J. Mater. Eng. Perform.* **18** 522–30

[78] Aurrekoetxea J, Zurbitu J, de Mendibil I O, Agirregomezkorta A, Sánchez-Soto M and Sarrionandia M 2011 Effect of superelastic shape memory alloy wires on the impact behavior of carbon fiber reinforced in situ polymerized poly(butylene terephthalate) composites *Mater. Lett.* **65** 863–5

[79] Zhou G and Lloyd P 2009 Design, manufacture and evaluation of bending behaviour of composite beams embedded with SMA wires *Compos. Sci. Technol.* **69** 2034–41

[80] Kang K W and Kim J K 2009 Effect of shape memory alloy on impact damage behavior and residual properties of glass/epoxy laminates under low temperature *Compos. Struct.* **88** 455–60

[81] Bollas D, Pappas P, Parthenios J and Galiotis C 2007 Stress generation by shape memory alloy wires embedded in polymer composites *Acta Mater.* **55** 5489–99

[82] Pinto F and Meo M 2015 Mechanical response of shape memory alloy–based hybrid composite subjected to low-velocity impacts *J. Compos. Mater.* **49** 2713–22

[83] Zheng Y, Cui L and Schrooten J 2005 Thermal cycling behaviors of a NiTiCu wire reinforced Kevlar/epoxy composite *Mater. Lett.* **59** 3287–90

[84] Khalili S M R, Shiravi M and Nooramin A S 2010 Mechanical behavior of notched plate repaired with polymer composite and smart patches—experimental study *J. Reinf. Plast. Compos.* **29** (19) 3021–37

[85] Davis B, Turner T L, Measurement S S and 2008 Prediction of the Thermomechanical Response of Shape Memory Alloy Hybrid Composite Beams *J. Intell. Mater. Syst. Struct.* **19** 129–43

[86] Boussu F, Bailleul G, Petitniot J C, Vinchon H and Warneton D 2002 Development of shape memory alloy fabrics for composite structures *Autex Res. J.* **2** 1–7

[87] Psarras G C, Parthenios J and Galiotis C 2001 Adaptive composites incorporating shape memory alloy wires Part I Probing the internal stress and temperature distributions with a laser Raman sensor *J. Mater. Sci.* **36** 535–46

[88] Jonnalagadda K D, Sottos N R, Qidwai M A and Lagoudas D C 1998 Transformation of Embedded Shape Memory Alloy Ribbons *J. Intell. Mater. Syst. Struct.* **9** 379–90

[89] Tsoi K A, Schrooten J, Zheng Y and Part S R 2004 Thermomechanical characteristics of shape memory alloy composites *Mater. Sci. Eng.* A **368** 299–310 II

[90] Aoki T and Shimamoto A 2003 Active Vibration Control of Epoxy Matrix Composite Beams with Embedded Shape Memory Alloy TiNi Fibers *Int. J. Mod. Phys.* **17** 1744–1749

[91] Yang B, Zhang Y, Xuan F Z, Xiao B, He L and Gao Y 2018 Improved adhesion between nickel–titanium SMA and polymer matrix via acid treatment and nano-silica particles coating *Adv. Compos. Mater.* **27** 331–48

[92] Jonnalagadda K, Kline G E and Sottos N R 1997 Local displacements and load transfer in shape memory alloy composites *Exp. Mech.* **37** 78–86

[93] Ogisu T, Shimanuki M, Kiyoshima S, Takaki J and Takeda N 2004 Damage suppression in CFRP laminates using embedded shape memory alloy foils *Adv. Compos. Mater.* **13** 27–42

[94] Amano M, Okabe Y and Takeda N 2005 Evaluation of Crack Suppression Effect of TiNi SMA Foil Embedded in CFRP Cross-Ply Laminates with Embedded Small-Diameter FBG Sensor *JSME Int. J. Ser.* A **48** 443–50

[95] Ogisu T, Shimanuki M, Kiyoshima S and Takeda N 2005 A Basic Study of CFRP Laminates with Embedded Prestrained SMA Foils for Aircraft Structures *J. Intell. Mater. Syst. Struct.* **16** 175–85

[96] Hiremath S R, Harish K, Vasireddi R, Benal M M and Mahapatra D R 2015 Effects of interface treatment on the fatigue behaviour of shape memory alloy reinforced polymer composites *Goulbourne NC, Editor. Behavior and Mechanics of Multifunctional Materials and Composites* Int. Society for Optics and Photonics. SPIE vol 9432 pp 198–202

[97] Arnaboldi S, Bassani P, Biffi C A, Tuissi A, Carnevale M and Lecis N *et al* 2011 Simulated and Experimental Damping Properties of a SMA/Fiber Glass Laminated Composite *J. Mater. Eng. Perform.* **20** 551–8

[98] Zhao L M, Feng X, jun Mi X, feng Li Y, feng Xie H and qian Yin X 2014 The interfacial strength improvement of SMA composite using ZnO with electrochemical deposition method *Appl. Surf. Sci.* **320** 670–3

[99] Fathi H, Shokrieh M M and Saeedi A 2019 A theoretical and experimental investigation on the stress distribution in the interface of pre-strained SMA wire/polymer composites *Compos. B: Eng.* **175** 107100

[100] Fathi H, Shokrieh M M and Saeedi A 2020 Effect of tensile loading rate on interfacial properties of SMA/polymer composites *Compos. B: Eng.* **183** 107730

[101] Zhang Y and Mi C 2020 Strengthening bonding strength in NiTi SMA fiber-reinforced polymer composites through acid immersion and Nanosilica coating *Compos. Struct.* **239** 112001

[102] Zak A J, Cartmell M P and Ostachowicz W 2003 Dynamics of Multilayered Composite Plates With Shape Memory Alloy Wires *J. Appl. Mechan.* **06;70** 313–27

[103] Sun M, Chang M, Wang Z, Li H, and Liu Y 2018 Simulation of Eccentric Impact of Square and Rectangular Composite Laminates Embedded with SMA *Materials (Basel)* **11** 2371

[104] Zaman I, Manshoor B, Khalid A, Araby S and bin Ghazali M I 2013 Vibration Characteristics of Composite Plate Embedded with Shape Memory Alloy at Elevated Temperature *Advances in Manufacturing and Mechanical Engineering of Applied Mechanics and Materials* Trans Tech Publications Ltd vol 393 pp 655–60

[105] Jang B K and Kishi T 2006 Influence of stacking angle of carbon fibers on fracture behavior of TiNi fiber impregnated CFRP composites *J. Alloys Compd.* **419** 208–12

[106] Wilkes K E and Liaw P K 2000 The fatigue behavior of shape-memory alloys *J. Minerals, Metals Mater. Soc. (JOM)* **52** 45–51

[107] El-Tahan M, Dawood M and Song G 2015 Development of a self-stressing NiTiNb shape memory alloy (SMA)/fiber reinforced polymer (FRP) patch *Smart Mater. Struct.* **24** 065035

[108] El-Tahan M and Dawood M 2015 Fatigue behavior of a thermally-activated NiTiNb SMA-FRP patch *Smart Mater. Struct.* **25** 015030

[109] Zheng B and Dawood M 2017 Fatigue crack growth analysis of steel elements reinforced with shape memory alloy (SMA)/fiber reinforced polymer (FRP) composite patches *Compos. Struct.* **164** 158–69

[110] Abdy A I, Hashemi M J and Al-Mahaidi R 2018 Fatigue life improvement of steel structures using self-prestressing CFRP/SMA hybrid composite patches *Eng. Struct.* **174** 358–72

[111] Zheng B T, El-Tahan M and Dawood M 2018 Shape memory alloy-carbon fiber reinforced polymer system for strengthening fatigue-sensitive metallic structures *Eng. Struct.* **171** 190–201

[112] Baz A, Imam K and McCoy J 1990 Active vibration control of flexible beams using shape memory actuators *J. Sound Vib.* **140** 437–56

[113] Baz A, Poh S, Ro J, Mutua M and Gilheany J 1992 ed Tzou H S and Anderson G L *Active Control of Nitinol-Reinforced Composite Beam* (Dordrecht: Springer, Netherlands) pp 169–212

[114] Turner T L 2002 Structural acoustic response of a shape memory alloy hybrid composite panel (lessons learned) Davis L P editor Smart Structures and Materials Smart Structures and Integrated Systems 4701 Int. Society for Optics and Photonics. SPIE 592–603

[115] Petr S, Michaud V, Modelling S J and 2002 Material Design of SMA Polymer Composites *MATERIALS TRANSACTIONS* **43** pg984–993

[116] Xu Y, Otsuka K, Toyama N, Yoshida H, Nagai H and Kishi T 2003 A novel technique for fabricating SMA/CFRP adaptive composites using ultrathin TiNi wires *Smart Mater. Struct.* **13** 196–202

[117] Faiella G, Antonucci V, Daghia F, Fascia S, Fabrication G M and 2011 Thermo-Mechanical Characterization of a Shape Memory Alloy Hybrid Composite *J. Intell. Mater. Syst. Struct.* **22** 245–52

[118] Kirkby E L, O'Keane J, de Oliveira R, Michaud V J and Manson J A E 2009 Tailored processing of epoxy with embedded shape memory alloy wires *Smart Mater. Struct.* **18** 095043

[119] Taheri-Behrooz F, Taheri F and Hosseinzadeh R 2011 Characterization of a shape memory alloy hybrid composite plate subject to static loading *Mater. Des.* **32** 2923–33

[120] Garcia E, Cudney H and Dasgupta A 1994 Adaptive structures and composite materials *Analysis and Application* American Society of Mechanical Engineers (ASME), Illinois, USA

[121] Pfaeffle H J, Lagoudas D C, Tadjbakhsh I G and Craig K C 1917 Design of flexible rods with embedded SMA actuators *Smart Structures and Materials 1993 Smart Structures and Intelligent Systems* ed Hagood N W and Knowles G J vol 1993 Int. Society for Optics and Photonics SPIE pp 762–73

[122] Paine J S N, Rogers C A and Smith R A 1995 Adaptive Composite Materials with Shape Memory Alloy Actuators for Cylinders and Pressure Vessels *J. Intell. Mater. Syst. Struct.* **6** 210–19

[123] Friend C M and Morgan N 1995 The Actuation Response of Model SMA Hybrid Laminates *J. Phys. IV France* **05** 415–20

[124] Song G, Kelly B and Agrawal B N 2000 Active position control of a shape memory alloy wire actuated composite beam *Smart Mater. Struct.* **9** 711–16

[125] Song S H, Lee H, Lee J G, Lee J Y, Cho M and Ahn S H 2016 Design and analysis of a smart soft composite structure for various modes of actuation *Compos. B: Eng.* **95** 155–65

[126] Lelieveld C, Jansen K and Teuffel P 2016 Mechanical characterization of a shape morphing smart composite with embedded shape memory alloys in a shape memory polymer matrix *J. Intell. Mater. Syst. Struct.* **27** 2038–48

[127] Kim M S, Chu W S, Lee J H, Kim Y M and Ahn S H 2011 Manufacturing of inchworm robot using shape memory alloy (SMA) embedded composite structure *Int. J. Precision Eng. Manuf.* **12** 565–8

[128] Hua Y, Ni Q Q, Yamanaka A, Teramoto Y and Natsuki T 2011 The Development of Composites with Negative Thermal Expansion Properties Using High Performance Fibers *Adv. Compos. Mater.* **20** 463–75

[129] Baz A M and Chen T H 1993 Performance of Nitinol-reinforced drive shafts *Smart Structures and Materials 1993 Smart Structures and Intelligent Systems* ed Hagood N W and Knowles G J vol 1917 Int. Society for Optics and Photonics SPIE pp 791–808

[130] Lau K T 2002 Vibration characteristics of SMA composite beams with different boundary conditions *Mater. Des.* **23** 741–9

[131] Baburaj V and Matsuzaki Y 1996 Material Damping Analysis of Smart Hybrid Composite Laminated Plate Structures *J. Intell. Mater. Syst. Struct.* **7** 427–32

[132] Bidaux J-E, Bernet N, Sarwa C, Manson J-A E and Gotthardt R 1995 Vibration Frequency Control of a Polymer Beam Using Embedded Shape-Memory-Alloy Fibres *J. Phys. IV France* **05** 1177–82

[133] Bidaux J E, Manson J A E and Gotthardt R 1996 Active modification of the vibration frequencies of a polymer beam using shape memory alloy fibres *Gobin PFP, Editor. Proc. of the SPIE, of Society of Photo-Optical Instrumentation Engineers (SPIE) Conf. Series* vol 2779 pp 517–22

[134] Malekzadeh K, Mozafari A and Ghasemi F A 2014 Free vibration response of a multilayer smart hybrid composite plate with embedded SMA wires *Latin Am. J. Solids Struct.* **03** 279–98

[135] Schetky L M, Liang C and Rogers C A 1994 Hybrid composite materials using shape memory alloy actuators to provide vibration and acoustic control *Smart Structures and Materials 1994 Smart Structures and Intelligent Systems* editor Hagood N W vol 2190 Int. Society for Optics and Photonics. SPIE pp 422–33

[136] Epps J and Chandra R 1997 Shape memory alloy actuation for active tuning of composite beams *Smart Mater. Struct.* **6** 251–64

[137] Gupta A K, Velmurugan R, Joshi M and Gupta N K 2019 Studies on shape memory alloy-embedded GFRP composites for improved post-impact damage strength *Int. J. Crashworthiness* **24** 363–79

[138] Kuang K S C and Cantwell W J 2003 The use of plastic optical fibres and shape memory alloys for damage assessment and damping control in composite materials *Meas. Sci. Technol.* **14** 1305–13

[139] Saeedi A and Shokrieh M M 2017 Effect of shape memory alloy wires on the enhancement of fracture behavior of epoxy polymer *Polym. Test.* **64** 221–8

[140] Zheng B T, El-Tahan M and Dawood M 2018 Shape memory alloy-carbon fiber reinforced polymer system for strengthening fatigue-sensitive metallic structures *Eng. Struct.* **171** 190–201

[141] Kirkby E L, Michaud V J, JAE Månson, Sottos N R and White S R 2009 Performance of self-healing epoxy with microencapsulated healing agent and shape memory alloy wires *Polymer* **50** 5533–8
[142] Karimi M, Bayesteh H and Mohammadi S 2019 An adapting cohesive approach for crack-healing analysis in SMA fiber-reinforced composites *Comput. Methods Appl. Mech. Eng.* **349** 550–75
[143] Sharma S, Nandan G, Rohatgi P and Prakash R 2019 Recent Advances Self-Healing Materials. Materials Today: Proc. *9th Int. Conf. of Materials Processing and Characterization, ICMPC-2019* vol 18 pp 4729–37
[144] Wang Y, Pham D T and Ji C 2015 Self-healing composites: A review *Cogent Eng.* **2** 1075686
[145] Poormir M A, Khalili S M R and Eslami-Farsani R 2018 Optimal design of a bio-inspired self-healing metal matrix composite reinforced with NiTi shape memory alloy strips *J. Intell. Mater. Syst. Struct.* **29** 3972–82
[146] Kessler M R 2007 Self-healing: A new paradigm in materials design *Proc. of the Institution of Mechanical Engineers, Part G: Journal of Aerospace Engineering* vol 221 pp 479–95
[147] Kirkby E L, Rule J D, Michaud V J, Sottos N R, White S R and Månson J A E 2008 Embedded Shape-Memory Alloy Wires for Improved Performance of Self-Healing Polymers *Adv. Funct. Mater.* **18** 2253–60
[148] Saeedi A and Shokrieh M M 2019 A novel self-healing composite made of thermally reversible polymer and shape memory alloy reinforcement *J. Intell. Mater. Syst. Struct.* **30** 1585–93
[149] Cui D, Song G and Li H 2010 Modeling of the electrical resistance of shape memory alloy wires *Smart Mater. Struct.* **19** 055019
[150] Nagai H and Oishi R 2006 Shape memory alloys as strain sensors in composites *Smart Mater. Struct.* **15** 493–8
[151] Senf B, Mader T, Sosa IN y de, Bucht A, Knobloch M and Löpitz D *et al* 2017 Sensing and Actuating Functions by Shape Memory Alloy Wires Integrated into Fiber Reinforced Plastics. Procedia CIRP *1st Conf. on Composite Materials Parts Manufacturing (CIRP CCMPM)* vol 66 pp 249–53
[152] xue Qiu Z, tian Yao X, Yuan J and Soutis C 2006 Experimental research on strain monitoring in composite plates using embedded SMA wires *Smart Mater. Struct.* **15** 1047–53
[153] Pinto F, Ciampa F, Meo M and Multifunctional P U 2012 SMArt composite material forin situNDT/SHM and de-icing *Smart Mater. Struct.* **21** 105010 aug
[154] Davis A, Mirsayar M and Hartl D 2019 Structural health monitoring using embedded magnetic shape memory alloys for magnetic sensing Gyekenyesi A L, editor Nondestructive Characterization and Monitoring of Advanced Materials, Aerospace, Civil Infrastructure, and Transportation XIII Int. Society for Optics and Photonics SPIE 10971 170–8
[155] Wang X, Liu H and Ouyang S 2008 Damping properties of flexible epoxy resin *J. Wuhan Univ. Technol. Mater. Sci. Ed.* **23** 411–14 Jun
[156] xin Zhang R, Ni Q Q, Natsuki T and Iwamoto M 2007 Mechanical properties of composites filled with SMA particles and short fibers *Compos. Struct.* **79** 90–6
[157] Lei H S, Zhou B, Wang Z Q and Wang X Q 2012 Tensile properties of random distribution short SMA fiber reinforced composites *Advances in Fracture and Damage Mechanics X of Key Engineering Materials* Trans Tech Publications Ltd vol 488 pp 686–9
[158] Lei H, Wang Z, Zhou B, Tong L and Wang X 2012 Simulation and analysis of shape memory alloy fiber reinforced composite based on cohesive zone model *Mater. Des.* **40** 138–47
[159] Murasawa G, Tohgo K and Ishii H 2004 Deformation behavior of NiTi/polymer shape memory alloy composites–experimental verifications *J. Compos. Mater.* **38** 399–416
[160] Birman V 2009 Effect of elastic or shape memory alloy particles on the properties of fiber-reinforced composites *J. Mech. Mater. Struct.* **4** 1209–25
[161] Raghavan J, Bartkiewicz T, Boyko S, Kupriyanov M, Rajapakse N and Yu B 2010 Damping, tensile and impact properties of superelastic shape memory alloy (SMA) fiber-reinforced polymer composites *Compos. B: Eng.* **41** 214–22
[162] Ni Q Q, xin Zhang R, Natsuki T and Iwamoto M 2007 Stiffness and vibration characteristics of SMA/ER3 composites with shape memory alloy short fibers *Compos. Struct.* **79** 501–7
[163] Khalili S M R, Shokuhfar A, Ghasemi F A and Malekzadeh K 2007 Dynamic response of smart hybrid composite plate subjected to low-velocity impact *J. Compos. Mater.* **41** 2347–70
[164] Wei L, Yu H, Yufeng L and Naibin Y 2013 Damping of Ni–Mn–Ga epoxy resin composites *Chin. J. Aeronaut.* **26** 1596–605
[165] Bielefeldt B R, Hochhalter J D and Hartl D J 2018 Shape memory alloy sensory particles for damage detection: Experiments, analysis and design studies *Struct. Health Monit.* **17** 777–814